

Chronic oxytocin improves neural decoupling at rest in children with autism: An exploratory RCT

Alaerts Kaat * ^{1,3} ×, Moerkerke Matthijs* ^{2,3}, Daniels Nicky* ^{1,3}, Zhang Qianqian^{1,3}, Grazia Ricchiuti ^{1,3}, Steyaert Jean³, Prinsen Jellina ^{1,3} †, Boets Bart^{2,3} †

* Joint first authors

† Joint senior authors

¹ KU Leuven, Neuromodulation Laboratory, Research Group for Neurorehabilitation, Leuven, Belgium.

² KU Leuven, Center for Developmental Psychiatry, Department of Neurosciences, Leuven, Belgium

³ KU Leuven, Leuven Autism Research (LAuRes), Leuven, Belgium

× *Corresponding author:*

Kaat Alaerts

KU Leuven, Neuromodulation Laboratory, Research Group for Neurorehabilitation, Tervuursevest 101 box 1501, 3001 Leuven, Belgium.

E-mail: kaat.alaerts@kuleuven.be

Tel.: +32 16 37 64 46

Short title: Oxytocin impacts neural decoupling at rest in autism

Author Contributions:

K.A.: conceptualization, methodology, investigation, data curation, validation, writing—original draft, writing—review and editing, visualization, project administration, funding acquisition;

M.M.: conceptualization, investigation, data curation, validation, writing—review and editing, project administration;

N.D.: conceptualization, investigation, data curation, validation, writing—review and editing, project

administration;

Z.Q.: methodology, data curation, validation, writing—review and editing;

G.R.: methodology, data curation, validation, writing—review and editing;

J.S.: supervision, validation, writing—review and editing, project administration, funding acquisition.

J.P.: supervision, methodology, investigation, data curation, validation, writing—review and editing, project administration;

B.B.: supervision, conceptualization, validation, writing—review and editing, funding acquisition.

All authors have read and agreed to the submitted/published version of the manuscript.

Competing Interest Statement: The authors declare no competing interests.

Number of Figures: **5**

Number of Tables: **1**

Contents of supplemental material:

Supplementary Methods & Results

Supplementary Figures: **3**

Abstract

Background. Shifts in peak frequencies of oscillatory neural rhythms are put forward as a principal mechanism by which cross-frequency coupling/decoupling is implemented in the brain. During active neural processing, functional integration is facilitated through transitory formations of ‘harmonic’ cross-frequency couplings, whereas ‘non-harmonic’ decoupling among neural oscillatory rhythms is postulated to characterize the resting, default state of the brain, minimizing the occurrence of spurious, noisy, background couplings.

Methods. Within this exploratory, randomized, placebo-controlled trial, we assessed whether the transient occurrence of non-harmonic and harmonic relationships between peak-frequencies in the alpha (8–14Hz) and theta (4–8Hz) bands is impacted by intranasal administration of oxytocin, a neuromodulator implicated in improving homeostasis and reducing stress/anxiety. To do so, resting-state electroencephalography was acquired before and after four weeks of oxytocin administration (12IU twice-daily) in children with autism spectrum disorder (8-12 years, $n=33$ oxytocin; $n=34$ placebo). At baseline, neural assessments of children with autism were compared with those of a matched cohort of children without autism ($n=40$).

Results. Compared to non-autistic peers, autistic children displayed a lower incidence of non-harmonic alpha-theta cross-frequency decoupling, indicating a higher incidence of spurious ‘noisy’ coupling in their resting brain ($p=.001$). Dimensionally, increased neural coupling was associated with more social difficulties ($p=.002$) and lower activity of the parasympathetic ‘rest & digest’ branch of the autonomic nervous system ($p=.018$), indexed with high-frequency heart-rate-variability. Notably, after oxytocin administration, the transient formation of non-harmonic cross-frequency configurations was increased in the cohort of autistic children ($p<.001$), indicating a beneficial effect of oxytocin on reducing spurious cross-frequency-interactions. Furthermore, parallel epigenetics changes of the oxytocin receptor gene indicated that the neural effects were likely mediated by changes in endogenous oxytocinergic signaling ($p=.006$).

Conclusions. Chronic oxytocin induced important homeostatic changes in the resting-state intrinsic neural frequency architecture, reflective of reduced noisy oscillatory couplings and improved signal-to-noise properties.

Keywords: Oxytocin; autism spectrum disorder; electroencephalography; heart rate variability, neural rhythms, alpha, theta, signal to noise

Key points and relevance

- Compared to their non-autistic peers, autistic children display reduced neural cross-frequency decoupling, indicative of more abundant noisy background oscillatory couplings among neural rhythms in their brain at rest.
- These alterations were mitigated through a four-week course of chronic oxytocin administration, normalizing their cross-frequency pattern to the one observed in children without autism.
- Low incidences of spurious, noisy couplings when the brain is at rest may lay the ground for a healthy intrinsic neural network which optimally prepares the system for transitions from rest to forthcoming active signal processing states.
- The observed effect of oxytocin on neural decoupling reflects an important mechanism by which oxytocin improves signal-to-noise properties of the intrinsic neural frequency architecture.

Introduction

The influence of oxytocin on social behaviors has garnered significant scientific and public interest in recent years. Oxytocin is a neuropeptide that plays a crucial role in modulating various complex social behaviors, including social reciprocity, attunement, social attachment, and stress regulation (Bartz et al., 2011). Intranasal administration of oxytocin is increasingly considered as a potential therapeutic option for various neuropsychiatric conditions, including autism spectrum disorders (ASD), due to its reported social and anxiolytic effects (Huang et al., 2021).

Endogenous oxytocin is synthesized in the hypothalamus where neurons of the paraventricular and magnocellular nuclei project to various areas of the central nervous system, including the amygdala, nucleus accumbens and frontal and temporal lobes (Jurek and Neumann, 2018, Wigton et al., 2015). Its widespread expression of receptors in both central brain regions and peripheral tissues, such as the heart, underscores its importance in homeostasis and stress regulation (Jurek and Neumann, 2018). As a neuromodulator, oxytocin has been implicated in various complex social behaviors, although the precise neural mechanisms underlying these effects remain incompletely understood. One theoretical account posits that oxytocin modulates social salience, enhancing social sensitivity (Shamay-Tsoory and Abu-Akel, 2016). Conversely, oxytocin has also been linked to regulation of central and autonomic homeostatic function, affecting (social) stress and anxiety responses (Stoop, 2012, Quintana and Guastella, 2020).

In addition, Owen et al. (2013) proposed that oxytocin may exert its complex neuromodulatory function by modulating the signal-to-noise properties of neural processes (Owen et al., 2013). In particular, they showed that oxytocin enhanced the signal-to-noise ratio of synaptic transmissions in the mammalian hippocampus by suppressing spontaneous neuronal firings, thereby facilitating efficient information transfer through increased fidelity of spike transmission. Similarly, an earlier study by Zaninetti & Raggenbass (2000) showed that oxytocin can exert strong facilitatory effects on spontaneous inhibitory post-synaptic currents in pyramidal cells, through increased release of the inhibitory neurotransmitter gamma-aminobutyric acid (GABA) from GABAergic interneurons (Zaninetti and Raggenbass, 2000). Subsequent studies have also demonstrated an impact of oxytocin on network oscillatory patterns, showing that oxytocin can suppress sharp wave-ripple complexes while increasing the temporal precision of oscillation-coupled spikes in mouse hippocampal tissue (Maier et al., 2016). Research in

rodents has also shown that oxytocin receptor activity in olfactory bulb neurons increases peak firing responses to social sensory information by lowering the baseline firing rate, thereby augmenting signal-to-noise properties for signal transmission (Oettl et al., 2016).

Prior human pharmaco-neuroimaging studies predominantly investigated oxytocin's neural effects using functional magnetic resonance imaging (fMRI) (Wigton et al., 2015, Grace et al., 2018, Fathabadipour et al., 2022), which offers high spatial precision, but limited temporal resolution. Studies adopting electroencephalographic (EEG) neuroimaging techniques which allow maximal temporal resolution are far more sparse, with only a handful of trials assessing oxytocin-induced changes in event-related potentials, EEG band power activity and microstates (de Bruijn et al., 2017, Peltola et al., 2018, Ruissen and de Bruijn, 2015, Waller et al., 2015, Ye et al., 2017, Festante et al., 2020, Wynn et al., 2019, Singh et al., 2016, Soriano et al., 2020, Rutherford et al., 2018, Van der Donck et al., 2022, Zhang et al., 2021, Schiller et al., 2019, Zelenina et al., 2022, Moerkerke et al., 2023).

EEG recordings of neural activity at the human scalp have revealed that neuronal populations exhibit firing patterns across discrete frequency bands (referred to as delta, theta, alpha, and beta bands) and synchronization of oscillatory activity across these distinct neural rhythms facilitates information transfer between neuronal cell populations across the brain (Fries, 2005, Roopun et al., 2008). The peak frequencies of neural oscillations have been proposed to act as a key mechanism for enabling cross-frequency coupling and decoupling in the brain (Klimesch, 2013, Klimesch, 2018, Rassi et al., 2019). This notion is rooted in the mathematical concept that neural oscillations can only achieve full synchronization when their peak frequencies constitute harmonic 2:1 relationships ($f_2 = f_1/2$; e.g. $f_1 = 10$ Hz and $f_2 = 5$ Hz), thereby allowing a pattern of frequent and regular excitatory phase meetings (Klimesch, 2013). In contrast, non-harmonic cross-frequency relationships based on the irrational golden mean 1.618:1 provide the highest physiologically possible desynchronized state, reducing the incidence of spurious, noisy, background coupling ($f_2 = f_1/1.6$; e.g. $f_1 = 10$ Hz and $f_2 = 6.18$ Hz) (Pletzer et al., 2010). As a result, the occurrence of non-harmonic cross-frequency patterns is thought to characterize the resting-state of the brain, during which no selective information processing takes place, as may be amplified through meditation or mindfulness practice (Rodriguez-Larios and Alaerts, 2020, Rodriguez-Larios et al., 2020b, Rodriguez-Larios et al., 2020a). The specific arrangement of adjacent EEG frequency bands generally concurs with a binary series of oscillatory rhythms, e.g. with $\delta = 2.5$, $\theta = 5$, $\alpha = 10$, $\beta = 20$, $\gamma = 40$, and state- and task-dependent shifts in peak frequencies have been

associated with transient shifts in harmonic/non-harmonic cross-frequency dynamics (Rodriguez-Larios and Alaerts, 2019, Rodriguez-Larios et al., 2020a, Rodriguez-Larios et al., 2020b, Rodriguez-Larios and Alaerts, 2020, Alaerts et al., 2021, Rassi et al., 2019).

In line with the signal-to-noise account of oxytocin, an initial study showed that the transient formation of non-harmonic cross-frequency decoupling configurations between alpha and theta peak frequencies is significantly increased after single-dose oxytocin administration (Alaerts et al., 2021). This indicates that, during resting-state, oxytocin reduces the intrinsic occurrence of spurious background phase synchronizations between alpha and theta rhythms implicated in memory and executive control (Rodriguez-Larios and Alaerts, 2020). Additionally, the same study showed single-dose oxytocin administration to enhance autonomic homeostasis and parasympathetic drive, as indexed by high-frequency heart rate variability (HRV), and baseline variations in HRV were associated to individual differences in non-harmonic cross-frequency arrangements. Altogether, this suggests that oscillatory systems with a low incidence of spurious cross-frequency couplings are reflected by a higher parasympathetic drive of the autonomic nervous system, which aligns with the notion that non-harmonic cross-frequency configurations lay the ground for a healthy neural network, allowing for an efficient transition from resting-state to activity (Pletzer et al., 2010, Rassi et al., 2019).

While these prior studies yielded important insights into oxytocin's neurophysiological effects to single-dose 'acute' administrations, insights in how multiple-dose 'chronic' repeated, daily administrations impact neural processes remain highly sparse with no study to date examining its temporal dynamics using EEG neurophysiological assessments. Particularly for autism, a neurodevelopmental condition characterized by difficulties in social interaction and (social) stress regulation (Cheng et al., 2020), an increasing number of chronic administration trials has emerged examining oxytocin's clinical-behavioral effects for relieving social difficulties. Yet, thus far, a mixed pattern of results has emerged, with some studies demonstrating beneficial clinical effects, while others did not (Horta et al., 2020, Huang et al., 2021). Pharmaco-neuroimaging of oxytocin's neural and stress physiological effects are urgently needed as it is anticipated that these assessments will allow for a more sensitive, objective evaluation of treatment effects and mechanisms, and may aid in understanding variation in its clinical-behavioral responses.

Here, we present an integrative investigation, examining how intrinsic, resting-state EEG cross-frequency dynamics among alpha and theta neural rhythms may differ in a cohort of school-aged autistic

children as compared to matched non-autistic peers, and particularly, whether children with autism may display reduced neural cross-frequency decoupling, indicative of more abundant noisy background oscillatory couplings among neural rhythms in their brain at rest.

Next, autistic children were enrolled in an exploratory, randomized, placebo-controlled trial examining how a four-week course of daily oxytocin administration (2 x 12 IU) may mitigate potential alterations in EEG cross-frequency dynamics in the cohort of children with autism. To examine whether the chronic oxytocin administration could induce long-lasting neurophysiological changes, EEG assessments were not only obtained immediately post-administration (24 hours after the last nasal spray administration), but also at a follow-up assessment, four weeks after cessation of the daily administrations. Following the prior single-dose oxytocin administration study (Alaerts et al., 2021), it was specifically explored whether the multiple-dose oxytocin administration regime could induce similar facilitatory effects on the formation of non-harmonic cross-frequency decoupling configurations among alpha and theta peak frequencies in the current pediatric cohort of autistic children.

To further our understanding into the effects of oxytocin on autonomic nervous system activity as well as the association among neural decoupling and autonomic homeostasis, we also obtained simultaneous high-frequency HRV recordings for investigating group differences and treatment outcomes in this established marker of cardiac, vagal parasympathetic activity, linked to psychophysiological homeostasis and well-being (Shaffer et al., 2014), i.e., similar to existing single-dose administration trials (Jain et al., 2017, Kemp et al., 2012, Alaerts et al., 2021, Martins et al., 2020, Norman et al., 2011).

Methods

Trial design and participants

The study encompassed a double-blind, randomized, placebo-controlled parallel design to perform an exploratory investigation into the neural and cardiac effects of four weeks of oxytocin administration in school-aged children with autism. Participants were enrolled in the trial to permit a 1:1 randomization strategy for two groups either receiving oxytocin or placebo nasal sprays (see **Figure 1** for the CONSORT flow diagram visualizing the number of participants randomized and **Table 1** for the number of participants analyzed: oxytocin: $n = 33$; placebo: $n = 34$, aged 10.49 ± 1.28 years, 13 girls). The autistic children underwent three neurophysiological assessment sessions: at baseline (T0); immediately post-administration (T1) (24 hours after the last nasal spray administration); and at a follow-up session, four weeks after cessation of the daily administrations (T2). To assess potential baseline diagnosis-related differences, a control group of children without a diagnosis of autism ($n = 40$, aged 10.28 ± 1.32 years, 8 girls, see **Table 1**) underwent a neurophysiological assessment at baseline (T0), but did not undergo any oxytocin or placebo nasal spray administration regime.

The study was conducted at the Leuven University Hospital (Leuven, Belgium) and was approved by the local Ethics Committee for Biomedical Research at the University of Leuven, KU Leuven (S61358) in accordance with The Code of Ethics of the World Medical Association (Declaration of Helsinki) (2013). The trial was registered at the European Clinical Trial Registry (EudraCT 2018-000769-35) and was part of a larger data collection, also including fMRI neuroimaging (Alaerts et al., 2023), frequency-tagging EEG (Moerkerke et al., 2023), biological sampling (Evenepoel et al., 2023, Moerkerke et al., 2024) and clinical-behavioral assessments (Daniels et al., 2023). As indicated in the trial registration, the EEG assessments were included as an exploratory outcome to examine the effects and neural mechanisms of oxytocin administration in autism.

Participants were recruited through the Leuven Autism Expertise Centre at the Leuven University Hospital and through elementary schools between July 2019 and January 2021. Autistic participants were eligible if they were diagnosed with ASD according to the Diagnostic and Statistical Manual of Mental Disorders, 5th edition (DSM-5) (APA, 1994), aged 8-12 years old, intelligence quotient above 70 and no prior oxytocin treatment. For each child, the formal ASD diagnosis was established by a multidisciplinary team (child psychiatrist and/or expert neuropediatrician, psychologist, speech/language

pathologist and/or physiotherapist). Individuals with any neurological disorder (stroke, concussion, epilepsy etc.), any physical disorder (liver, renal, cardiac pathology), significant hearing or vision impairments, or any neuropsychiatric diagnosis (only for control group) were excluded. Boys and premenstrual girls were included. As outlined in **Table 1**, children with autism were administered the Autism Diagnostic Observation Schedule, 2nd edition (ADOS-2) (Lord et al., 1999). For all children, the parent-rated Social Responsiveness Scale-Children, 2nd edition (SRS-2) (Constantino et al., 2003) and estimates of intelligence (Wechsler Intelligence Scale for Children, Fifth Edition, Dutch version; WISC-V-NL (Wechsler, 1999)) were acquired. Performance intelligence quotient (IQ) was derived from the subtests Block design and Figure puzzles and verbal IQ from the subtests Similarities and Vocabulary.

Medication schedules

Participants were randomized to receive oxytocin (Syntocinon®, Sigma-tau) or placebo nasal sprays, as prepared at the University Hospital of Heidelberg (Germany) in identical 10 ml glass bottles with a metered pump (0.05 ml or 2 IU /puff). Participants were asked to administer the nasal spray twice daily: 12 IU in the morning (3 puffs of 2 IU in each nostril) and 12 IU in the afternoon (after school). To monitor nasal spray compliance, the total amount of administered fluid was assessed (see **Supplementary Methods** and (Daniels et al., 2023)).

EEG recording and preprocessing

Recording. An ActiveTwo BIOSEMI acquisition system was used to collect continuous 5-minute resting-state EEG recordings with 64 Ag/AgCl scalp-electrodes. Two additional electrodes functioned as reference and ground electrodes (Common-Mode-Sense active electrode and Driven-Right-Leg passive electrode). Sampling rate for the digitized EEG-signal was 512 Hz. During the resting-state recording, children were instructed to relax, not think of anything in particular, and to avoid movement while fixating on a cross.

Preprocessing. Data preprocessing was performed using MATLAB R2021b and EEGLab (MATLAB version r2021b). Raw EEG data were filtered using a high- (1 Hz) and low-pass filter (40 Hz) prior to digitization. To improve computing speed, data were resampled to 250 Hz. Flat channels were detected and removed (clean flatlines), and artifact subspace reconstruction (asr) was applied to remove residual

artificial signal. Noisy channels were interpolated. Subsequently, artifacts of eye movement were removed using independent component analysis (ICA). Offline mathematical referencing was performed using current source density (CSD) transformation (Tenke and Kayser, 2005). For subsequent analyses, electrode recordings were clustered into 11 electrode clusters encompassing left and right frontal, central, parietal and occipital regions, as well as a midline frontal, central and occipital cluster (see **Figure 2, panel D**).

Transient peak detection and determination of cross-frequency relationships

The time-frequency representation of the EEG data was obtained using short-term Fast Fourier Transform (STFFT), computed using the MATLAB spectrogram function (Hanning window length of 1 sec and sliding step of 25 bins; i.e. 90.23 % overlap), with a frequency precision of 10 points per frequency (i.e. from 1 Hz until 40 Hz in 400 frequency lines). Then, transient peak frequencies of the theta (4–8 Hz) and alpha (8–14 Hz) bands were detected for each (overlapping) 1 sec epoch of transformed data using the find local maxima function implemented in MATLAB r2020b (i.e. findpeaks) (similar to procedures described in (Rodriguez-Larios and Alaerts, 2019)). Using this algorithm, data samples larger than their two neighboring samples were identified as local peaks within the specified alpha and theta frequency ranges. Based on the identified peak frequencies, the numerical ratio of the alpha and theta peaks ($\text{peak-frequency}_{\text{alpha}} / \text{peak-frequency}_{\text{theta}}$) was calculated for each epoch and rounded to the first decimal place (e.g., 10/5 Hz = 2.0). Hence, the obtained ratio-values ranged between 1.1 and 3.4 in steps of 0.1. When two or more peaks were detected in one frequency band, only the peak with highest amplitude was selected. For a limited number of epochs, no clear peaks were detected in the theta or alpha bands and were excluded from further analyses (in the autism group: 4.30 % at T0; 4.40% at T1; and 4.33% at T2, across electrodes and participants) (in the control group: 4.45% at T0).

Figure 2A visualizes the transient (epoch-wise) variability of alpha and theta peak frequencies over time (i.e. 10 sec) for an exemplary subject and electrode, as well as the transient numerical ratio over time.

Figure 2B visualizes the FFT frequency spectra of two exemplary epochs in which the identified alpha and theta peak frequencies formed a 'harmonic' (2:1) versus a 'non-harmonic' (1.6:1) cross-frequency relationship (partly adapted from (Rodriguez-Larios and Alaerts, 2019)). **Figure 2C** visualizes the distribution of the percentage occurrence of all possible ratios, as recorded at baseline (before nasal

spray administration). In line with Rodriguez et al. (2019, 2020) (Rodriguez-Larios and Alaerts, 2019, Rodriguez-Larios et al., 2020a) and Alaerts et al. (2021) (Alaerts et al., 2021), the distribution showed a maximal occurrence of the non-harmonic 1.6:1 alpha:theta ratio aspect (9.46 %, average across electrodes), indicating that this configuration forms a highly prevalent physiological state within the intrinsic resting-state EEG frequency architecture. The harmonic 2:1 ratio aspect showed an average occurrence of 6.86%. For subsequent analyses, the proportion of epochs in which the alpha:theta peak ratio equaled 1.6:1 or 2.0:1 (termed non-harmonic 'decoupling' and harmonic 'coupling') was determined for each electrode cluster.

Heart rate variability recording and data handling

Photoplethysmography (PPG) recordings were performed simultaneous to the resting-state EEG (5 min session) using the ActiveTwo BIOSEMI multimodal acquisition system at a sampling rate of 512 Hz. The PPG pulse oximeter sensor was placed over the ring finger of the non-dominant hand to monitor blood volume changes in the microvascular bed of the underlying tissue. The time intervals between blood volume pulse waves were assessed using Kubios HRV Premium software (version 3.2) (Tarvainen et al., 2014) to derive continuous inter-beat-intervals for assessing heart rate variability (HRV). All inter-beat-interval time series were manually inspected prior to analysis and automatic artifact removal, as implemented in Kubios HRV, was performed.

At T0, PPG recordings were acquired for 93 participants (30 control/65 autism) of which 83 (30 control/53 autism) passed quality control (availability of 5 min of noise-free data and/or less than 5% ectopic beats (Laborde et al., 2017)). Of the autism group with qualitative T0 baseline recordings, HRV recordings with quality control were obtained from 47 participants (24 oxytocin/23 placebo) at T1 and from 46 participants (24 oxytocin/22 placebo) at T2. For each subject and session (T0, T1, T2), HRV frequency domain analyses were performed using Fast Fourier Transformation (FFT) based on Welch's periodogram to compute HRV band power using the power spectral density of the detrended inter-beat-interval series as implemented in the Kubios HRV Premium software. For completeness, both high-frequency (0.15–0.4 Hz, % relative power, see main results) and low-frequency HRV band power were computed (0.04-0.15 Hz, see **Supplementary Results**).

Statistical analysis

All statistics were performed using Statistica version 14 (Tibco Software Inc.).

Assessment of diagnostic-related group differences. To assess diagnostic-related differences between children with and without autism in alpha-theta cross-frequency relationships, the proportion of epochs that displayed 1.6:1 non-harmonic decoupling and 2:1 harmonic coupling, were subjected to mixed-effect analyses with the random factor 'subject' and the fixed factors 'diagnostic group' (autism, control), 'cross-frequency ratio' (1.6 and 2.0) and 'electrode cluster' (11 clusters). Diagnosis-related differences in high-frequency HRV were assessed using independent-samples t-tests.

Assessment of oxytocin-induced changes. Oxytocin-induced effects were analyzed using an intention-to-treat format with last-observations-carried-forward to replace missing data. For participants with missing baseline data, data for that measure were excluded list-wise. See the Consort flow diagram in **Figure 1** for the included EEG data. For the high-frequency HRV data, analyses were performed on a total of 27 oxytocin (3 imputed) and 23 placebo participants (1 imputed at T2). Note that EEG and HRV analyses, conducted on data without imputation rendered a similar pattern of results (see **Supplementary Results**).

For each ratio, pre-to-post change scores were calculated and subjected to mixed-effect analyses with the random factor 'subject' and the fixed factors 'nasal spray' (oxytocin, placebo), 'assessment session' (T1, T2), 'cross-frequency ratio' (1.6 and 2.0) and 'electrode cluster' (11 clusters). Oxytocin-induced effects in high-frequency HRV were assessed using similar mixed-effect analyses, with the random factor 'subject' and the fixed factors 'nasal spray' (oxytocin, placebo) and 'assessment session' (T1, T2).

Significant interaction effects, emerging from the mixed effect analyses were further explored using lenient Fisher LSD post-hoc tests, as well as more stringent post-hoc analyses with Bonferroni correction for multiple comparisons.

Baseline variations. Spearman correlation analyses were performed to explore whether baseline variations in EEG cross-frequency ratio aspects were associated with high-frequency HRV as well as with social difficulties (SRS-2 total scores) in the autism group.

Associations of oxytocin-induced changes in EEG to changes in high-frequency HRV and behavior. To examine whether variations in the extent of oxytocin-related effects on EEG cross-frequency were associated to oxytocin-induced changes in high-frequency HRV or social difficulties (SRS-2 total

scores), Spearman correlation analyses were performed between change-from-baseline scores separately for the T1 and T2 assessment session.

Associations of oxytocin-induced changes in EEG and high-frequency HRV to changes in biological sampling parameters. Further, as mentioned above, the current neural and cardiac characterizations were part of a larger assessment protocol, also including biological sampling assessments of oxytocin signaling, including changes in endogenous salivary oxytocin and epigenetics of the oxytocin receptor gene (*OXTR*). Specifically, as reported in Moerkerke et al. (2024), the four-week oxytocin administration regime was shown to elicit a significant rise in endogenous oxytocin levels (most pronounced for morning salivary samples, assessed at T1), as well as a reduction in *OXTR* methylation (particularly at CpG site -924), indicative of increased receptor expression (Moerkerke et al., 2024). Here, we examined whether the extent of oxytocin-related effects on EEG cross-frequency and high-frequency HRV were associated to oxytocin-induced changes in these biological sampling parameters (oxytocin hormonal levels and *OXTR* methylation) (see **Supplementary Methods** and (Evenepoel et al., 2023, Moerkerke et al., 2024) for more information on the assessment procedures). Considering their exploratory nature, Spearman correlation analyses are reported at a $p < .05$ uncorrected statistical threshold.

Finally, to obtain deeper insight in the mechanistic process of oxytocin-induced modulations in cross-frequency coupling, secondary EEG analyses were performed examining changes in alpha and theta peak frequencies and amplitudes as reported in **Supplementary Methods and Results**.

Results

Diagnosis-related differences in EEG and HRV at baseline

EEG cross-frequency dynamics. Mixed-effects analysis showed a significant main effect of 'cross-frequency ratio' indicating that irrespective of diagnostic group, the non-harmonic 1.6:1 ratio aspect (reflective of cross-frequency decoupling) displayed a higher occurrence, compared to the harmonic 2:1 ratio aspect (reflective of cross-frequency coupling) ($F(1, 2205) = 6970.17; p < .001$) (**Figure 2C**). Mixed-effects analysis also showed a significant 'diagnostic group x cross-frequency ratio' interaction ($F(1, 2205) = 30.57; p < .001$), indicating a significantly lower occurrence of non-harmonic 'decoupling' 1.6:1 ratio aspects in the autistic compared to the control group (post-hoc: $p_{Fisher\ LSD} < .001; p_{Bonferroni} = .0012$), and a significantly higher occurrence of harmonic 'coupling' 2:1 ratio aspects in the autistic compared to the control group ($p_{Fisher\ LSD} < .001; p_{Bonferroni} < .001$) (**Figure 3A**). While the effect was evident across clusters, the three-way 'diagnostic group x cross-frequency ratio x cluster' interaction indicated that the diagnostic effect on non-harmonic ratios was most pronounced for the left central cluster, whereas the harmonic ratio effect was most pronounced for the right occipital cluster ($F(20, 2205) = 5.41; p < .001$) (see **Supplementary Figure 1**, visualizing the diagnostic effect separately for each cluster).

High-frequency HRV. As a group, high-frequency HRV was not significantly different between children with and without autism ($t(81) = 1.24; p = .22$) (**Supplementary Figure 2**).

EEG x high-frequency HRV relationship. Spearman correlation analyses revealed a significant negative relationship between baseline recorded high-frequency HRV and the occurrence of the harmonic 2:1 ratio aspect (averaged across clusters), indicating that autistic children with a high extent of 2:1 cross-frequency coupling display lower parasympathetic vagal tone ($\rho = -.33; p = .018$) (**Figure 3B**). A trend-level opposite relationship was evident for the non-harmonic 1.6:1 ratio aspect, indicating higher parasympathetic high-frequency HRV in children with a higher presence of the non-harmonic 'decoupling' 1.6:1 ratio aspect in their brain at rest ($\rho = .24; p = .084$) (**Figure 3B**).

EEG x behavior relationship. Further, also a significant dimensional brain-behavior relationship was evident, indicating that autistic children with more pronounced social difficulties (higher scores on the Social Responsiveness Scale, SRS), displayed an overall lower occurrence of the non-harmonic 'decoupling' 1.6:1 ratio aspect (averaged across clusters) (Spearman $\rho = -.25; p = .039$) and a higher occurrence of the harmonic 'coupling' 2:1 ratio aspect ($\rho = .36; p = .002$) (**Figure 3C**).

Oxytocin-induced changes in EEG and HRV

EEG cross-frequency dynamics. Mixed-effect analyses identified a significant 'nasal spray x cross-frequency ratio x session' interaction ($F(1, 2795) = 8.46; p < .001$), indicating a differential effect of oxytocin on non-harmonic 1.6:1 and harmonic 2:1 ratio occurrences immediately post (T1) and at the four-week follow-up session (T2). Post-hoc analysis indicated that across all electrode clusters, children receiving oxytocin displayed a significant increase in the occurrence of the non-harmonic 'decoupling' 1.6:1 ratio aspect, compared to children receiving the placebo nasal spray, but only at the T2 four-week follow-up session ($p_{Fisher\ LSD} < .001; p_{Bonferroni} < .001$), not at the T1 session ($p_{Fisher\ LSD} = .96; p_{Bonferroni} > 1.0$) (**Figure 4A**). An opposite effect of nasal spray was evident for the harmonic 'coupling' 2:1 ratio aspect, indicating a reduced occurrence in the oxytocin group, compared to the placebo group at follow-up session T2 (post-hoc: $p_{Fisher\ LSD} = .014; p_{Bonferroni} = .40$), not at T1 (post-hoc: $p_{Fisher\ LSD} = .28; p_{Bonferroni} > 1.0$) (**Figure 4A**). Together, these results partly replicate findings from the prior single-dose administration study, where immediate 'acute' effects of oxytocin on EEG cross-frequency dynamics were evident (Alaerts et al., 2021). Here, the chronic oxytocin administration regime appeared to induce late-emerging effects on harmonic/ non-harmonic cross-frequency coupling, as evident at the T2 follow-up assessment, but not at the immediate T1 post assessment.

High-frequency HRV. Mixed-effect analyses of pre-to-post changes in high-frequency HRV revealed a significant 'nasal spray x session' interaction ($F(1, 48) = 4.77; p = .034$), indicating that, compared to the placebo group, children receiving oxytocin displayed significantly higher high-frequency HRV at the T1 post session, compared to the placebo group, (post-hoc: $p_{Fisher\ LSD} = .015; p_{Bonferroni} = .091$) (**Figure 4B**). However, the effect did not persist until the T2 follow-up session, four weeks after cessation of the nasal sprays (post-hoc: $p_{Fisher\ LSD} = .57; p_{Bonferroni} > 1.0$).

EEG x high-frequency HRV relationship. While as a group, participants of the oxytocin group displayed significant changes both in terms of high-frequency HRV and cross-frequency ratio aspects, correlation analyses revealed no significant relationships between the extent of pre-to-post changes in high-frequency HRV and the extent of pre-to-post changes in the occurrence of the (non-)harmonic ratio aspect, either at the T1 or T2 session (all, $p > .05$). Also correlation analyses directly assessing relationships between the extent of (late-emerging) changes, i.e., from the post (T1) to the one-month follow-up (T2), revealed no significant association between T1-to-T2 changes in the EEG ratio aspects and HRV (all, $p > .05$).

EEG x behavior relationship. In terms of associations with behavior, correlation analyses between the extent of pre-to-post changes in SRS scores and the extent of pre-to-post changes in the occurrence of the (non-)harmonic ratio aspect showed no significant relationships, either at the T1 or T2 session (all, $p > .05$). Interestingly, correlation analyses, directly assessing relationships between the extent of (late-emerging) changes, i.e., from the post (T1) to the one-month follow-up (T2), revealed significant brain-behavior relationships between T1-to-T2 changes in SRS scores and T1-to-T2 changes in the occurrence of both the non-harmonic ($\rho = -.44$; $p = .011$) and harmonic ratio aspect ($\rho = .38$; $p = .032$) (**Supplementary Figure 3**). In line with the identified baseline associations, the relationship indicated that participants with stronger late-emerging oxytocin-induced increases in 1.6:1 non-harmonic cross-frequency coupling, and stronger late-emerging decreases in 2:1 harmonic cross-frequency coupling (from T1 to T2), showed more pronounced improvements in social function (from T1 to T2).

Association between oxytocin-induced changes in neural/cardiac and biological sampling parameters

Previously, the four-week oxytocin administration regime was shown to elicit significant changes in oxytocinergic signaling, indicative of a rise in endogenous oxytocin levels and a reduction in *OXTR* methylation (indicative of elevated receptor expression) (Moerkerke et al., 2024). These biological changes in oxytocin levels and epigenetics were associated to the here observed neural/cardiac changes in the following way.

Pertaining to oxytocin-induced changes in *OXTR* methylation at CpG site -924, a significant association was identified with neural cross-frequency changes, indicating that participants of the oxytocin group with a stronger pre-to-post increase in the occurrence of the non-harmonic 'decoupling' 1.6:1 ratio aspect at T1, showed a stronger reduction in *OXTR* methylation, indicative of higher oxytocin receptor expression ($\rho = -.47$; $p = .006$) (**Figure 5A**). At the T2 follow-up session, the effect was no longer significant ($\rho = -.27$; $p = .12$) (**Figure 5A**). Also no significant associations were evident between *OXTR* methylation and high-frequency HRV (all, $p > .05$).

In terms of salivary oxytocin levels, a significant association was evident with the extent of changes in high-frequency HRV, indicating that participants of the oxytocin group with a strong retention of elevated high-frequency HRV at follow-up session T2, also showed a strong retention of elevated oxytocin levels ($\rho = .69$; $p < .001$) (**Figure 5B**). No significant associations were evident however,

between high-frequency HRV and endogenous oxytocin levels at the T1 immediate post session, or between oxytocin levels and neural cross-frequency changes (all, $p > .05$).

Discussion

Autistic children displayed a differential pattern of intrinsic, harmonic and non-harmonic cross-frequency interactions between alpha and theta neural rhythms, indicative of an increased incidence of neural coupling, and a reduced incidence of neural decoupling. This suggests that the resting autistic brain displays more 'noisy' background oscillatory couplings and may therefore be less 'at rest' as compared to the brain of non-autistic peers. Dimensionally, the increased incidence of neural coupling in the resting brain was associated with a higher expression of social difficulties (SRS) and lower 'rest and digest' parasympathetic activity of the autonomic nervous system, as measured using high-frequency HRV.

Importantly, in the cohort of children with autism, a four-week course of daily oxytocin administrations induced a relative increase in the incidence of non-harmonic alpha-theta cross-frequency interactions, thereby facilitating a shift of their intrinsic EEG cross-frequency architecture towards the pattern seen in non-autistic children, albeit note that the effect was late-emerging, four weeks after cessation of the last nasal spray. Furthermore, these neural changes were associated with changes in endogenous oxytocinergic signaling, in terms of epigenetic changes of the oxytocin receptor gene, rendering higher oxytocin receptor availability.

Neural rhythms do not exist in isolation but interact with one another for integrating their associated functions, e.g. among theta and alpha neural rhythms, implicated in executive and memory processes (Klimesch, 2018, Klimesch, 2012). By transiently shifting their peak frequencies, neural oscillators can align with each other in harmonic or non-harmonic configurations for maximizing or minimizing their excitatory phase meetings, i.e., facilitating cross-frequency coupling and cross-frequency decoupling (Klimesch, 2018, Pletzer et al., 2010). Generally, the formation of non-harmonic cross-frequency configurations, precluding the occurrence of 'noisy', unwanted, spurious couplings, has been associated with a healthy resting-state neural network allowing efficient transitions from resting-state to activity, increasing the signal-to-noise properties of the intrinsic EEG neural frequency architecture (Klimesch, 2018, Alaerts et al., 2021). Hence, during resting states, the brain's intrinsic neural circuitry may adjust its frequency architecture to a state in which cross-frequency decoupling is actively facilitated (at non-harmonic ratio 1.6:1) to avoid spurious phase synchronization. Conversely, during active cognitive task demands, the brain's neural circuitry may adjust its frequency architecture to a state in which cross-frequency coupling (harmonic ratio 2:1) is facilitated, allowing for enhanced information transfer for

neural processing.

In line with this notion, recent studies have shown that the occurrence of harmonic cross-frequency arrangements (2:1) between theta and alpha rhythms is most prominent during active cognitive processing, whereas the formation of non-harmonic arrangements (1.6:1) is more prominent during rest as well as during breath-focused meditation conditions (Rodriguez-Larios and Alaerts, 2019, Rodriguez-Larios and Alaerts, 2020, Rodriguez-Larios et al., 2020a). For example, pre-to-post increases in the occurrence of non-harmonic cross-frequency arrangements (1.6:1) were observed after an 8-week mindfulness training course, indicating a facilitation of the preclusion of unwanted spurious interactions among theta and alpha neural rhythms upon meditation practice (Rodriguez-Larios et al., 2020b).

In the current study, an initial investigation into the incidence of harmonic/non-harmonic cross-frequency interactions in pediatric populations with and without autism showed a significantly lower incidence of non-harmonic 1.6:1 alpha-theta cross-frequency relationships and a higher incidence of harmonic 2:1 interactions in the resting brain of autistic children. These results provide a first indication that - in terms of cross-frequency interactions - the signal-to-noise properties of the intrinsic EEG neural frequency architecture may be lower in autistic versus non-autistic children. These observations align with and extend recent empirical evidence of imbalances between excitatory and inhibitory (E/I) cortical activity in the autistic brain (Rubenstein and Merzenich, 2003, Bruining et al., 2020). The theoretical framework of the E/I imbalance model of autism proposes that reduced inhibition through the inhibitory neurotransmitter gamma-aminobutyric acid (GABA) in the brain of individuals with autism may lead to an increase in 'neural noise' and therefore a decrease in the signal-to-noise ratio of neural processes (Rubenstein and Merzenich, 2003). Overall, this imbalance in excitatory/inhibitory activity has been linked to aberrant sensory processing as frequently observed in autism, reflective of an imbalance in filtering sensory information from the external surroundings (Mazurek et al., 2013, APA, 2013). In turn, the development of repetitive and restricted behaviors has been suggested to constitute a coping mechanism, serving the individual to make the influx of complex environmental information more predictable (Van de Cruys et al., 2014). Also withdrawal from social situations, resulting eventually in social difficulties, may initially represent an adaptive response to avoid the complexity and unpredictability of social interactions (Johnson, 2017). In the present study, and aligning with this notion, inter-individual variations in social difficulties were shown to be associated with differential patterns of harmonic/non-harmonic cross-frequency relationships. Specifically, a lower incidence of non-harmonic

cross-frequency interactions, indicative of a higher incidence of noisy, spurious cross-frequency couplings and putatively lower signal-to-noise balance, was associated with a higher expression of social difficulties.

Importantly, and in line with a recent single-dose administration study (Alaerts et al., 2021), our four-week course of daily oxytocin administrations yielded a significant increase in the transient formation of non-harmonic cross-frequency configurations in children with autism. Note however, that the observed changes upon the chronic administration constituted a late-emerging effect, observed at the four-week follow-up assessment (T2), but not immediately after the four-week administration regime (T1). Interestingly, it appeared that the extent of these late-emerging oxytocin-induced changes in (non-)harmonic cross-frequency interactions (from T1 to T2) were significantly associated with improvements in social function (from T1 to T2). These observations align with the identified baseline associations with social symptom severity, and highlight that the observed oxytocin-induced mitigation of altered cross-frequency interactions in autistic children, i.e., towards patterns seen in non-autistic children, also dimensionally relates to clinical-behavioral improvements in social difficulties.

In comparison with the previous acute dosing study (Alaerts et al., 2021), it appears that while the direction of 'trait-like' chronic and 'state-like' acute effects on cross-frequency interactions is similar, the chronic administration regime appeared to show a different, more belated time course, with changes only fully emerging four weeks after cessation of the daily nasal spray administrations. Thus, while each acute dosing may have facilitated a reduction in intrinsic incidence of noisy, spurious cross-frequency couplings, likely relieving the individual from lower signal-to-noise or E/I imbalance, it appears that a trait-like consolidation of these short-lived, state-dependent changes was not yet evident at the immediate post assessment (i.e. performed 24 hours after the last nasal spray administration), but instead displayed a late-emergence, as evident at the four-week follow-up. Speculatively, the biological pathways through which oxytocin exerts its acute 'state-related' and chronic 'trait-related' effects may be qualitatively different, with the former depending on the heightened availability of the exogenously administered oxytocin, while the latter may depend more on late-emerging changes in the endogenous oxytocinergic system itself, potentially including (epi)genetic modifications impacting endogenous oxytocin signaling, e.g. in terms of oxytocin receptor expression. Examination of this possibility through the association analyses confirmed that neural oxytocin-induced changes in non-harmonic cross-frequency configurations were paralleled by oxytocin-induced changes in methylation of the *OXTR* (see

(Moerkerke et al., 2024)). Specifically, the association indicated that children displaying stronger oxytocin-induced reductions in *OXTR* methylation - facilitating higher oxytocin receptor expression – also showed stronger neural changes. Accordingly, it is speculated that the observed changes in oxytocinergic signaling may have been instrumental in facilitating the (late-emerging) neural changes in cross-frequency dynamics.

Both in the present study and in prior studies (Alaerts et al., 2021), baseline variations in intrinsic cross-frequency coupling/decoupling were associated to respectively, higher/lower high-frequency HRV, an established marker of parasympathetic autonomic nervous system activity. Prior single-dose oxytocin administration studies have linked oxytocin's acute facilitatory effects on HRV markers to its homeostatic role in balancing intrinsic parasympathetic vagal tone (Jain et al., 2017, Kemp et al., 2012, Alaerts et al., 2021, Martins et al., 2020, Norman et al., 2011). In line with these acute dosing studies, a boosting impact of the chronic oxytocin regime on high-frequency HRV was observed, indicating a facilitation of stress-regulatory, parasympathetic activity immediately after the oxytocin administration regime (T1), but no longer at the four-week follow-up session (T2). It is of note that despite their strong baseline relationships, it appeared that the time course of oxytocin-induced effects was different for neural and cardiac parameters, with the effects of high-frequency HRV emerging early, at the T1 assessment, whereas the cross-frequency changes showed a late emergence at the T2 follow-up assessment. Interestingly, however, it appeared that for a subset of children displaying sustainably elevated levels of endogenous oxytocin (as measured via saliva samples), elevated high-frequency HRV also persisted at the T2 follow-up session. No significant associations were evident, however, between changes in high-frequency HRV and epigenetic changes, as was observed for the neural changes. In this view, it is hypothesized that the pathways underlying oxytocin's effects on cardiac versus EEG neural effects may be qualitatively different, with the former relying predominantly on changes in the availability of circulating oxytocin and the latter depending more strongly on epigenetic changes in oxytocin signaling, thereby impacting receptor availability.

While the current study provides important new insights into diagnosis-related and oxytocin-induced changes in neural cross-frequency dynamics, the following limitations and recommendations are noted. First, the current study included a relatively tight age range of school-aged children with autism (aged 8-12 years), i.e., chosen to be similar to (Parker et al., 2017). While this tight age range constitutes an asset for improving homogeneity within the studied cohort, it reduces generalizability of the observed

effects to other age groups. Considering growing evidence that intranasal oxytocin may be most effective for autistic children under 5 years of age (e.g., see (Guastella et al., 2023)), future trials should explore whether the observed neurophysiological effects of oxytocin can be replicated in cohorts of younger children and/or autistic adults and adolescents. It is also unclear whether effects will generalize to cohorts with a larger representation of girls or women with autism, considering prior observations of differential oxytocin effects depending on biological sex (Wigton et al., 2015). Further, our study found oxytocin-related changes in non-harmonic/harmonic alpha-theta cross-frequency decoupling/coupling that were widespread across the scalp, indicating that the observed state or trait-dependent changes in cross-frequency interactions were evident at a broad spatial scale (similar to (Alaerts et al., 2021)). It would be valuable for future research to further explore the spatial distribution and/or source localization of the observed effects and to extend investigations to other cross-frequency relationships, e.g. between alpha and beta bands. Finally, in the current study, oxytocin's effects were examined on recordings of intrinsic, resting-state cross-frequency dynamics. It is therefore unclear whether the observed reductions in neural decoupling are specific to intrinsic, task-free contexts, or whether they will generalize to task-contexts requiring explicit social, affective or cognitive processing. Future research may be warranted to further explore the role of task-context in oxytocin's neurophysiological effects.

To conclude, important diagnosis-related differences were identified in the occurrence of harmonic and non-harmonic cross-frequency coupling and decoupling between alpha and theta neural rhythms, indicative of reduced signal-to-noise properties of neural processes in autistic versus non-autistic children. In children with autism, chronic oxytocin administration over a four-week course facilitated a long-lasting change in the pattern of cross-frequency configurations, normalizing them towards the pattern observed in children without autism. These observations provide important initial evidence that chronic oxytocin administration can induce trait-like changes in the signal-to-noise properties of the intrinsic neural frequency architecture.

Acknowledgements

We would like to thank all the participants of the study and our colleagues of the Leuven Autism Research Consortium (LAuRes).

This work was supported by a KU Leuven grant (C14/17/102), and Small Research Equipment fund of the KU Leuven (ELG-D2857) granted to K.A. and B.B.; a Doctor Gustave Delpont fund of the King Baudouin Foundation (2019-J1811190-212989) and the Branco Weiss fellowship of the Society in Science – ETH Zurich granted to K.A.; the Excellence of Science grant granted to B.B. (EOS; G0E8718N; HUMVISCAT) and a TBM grant of the Flanders Fund for Scientific Research (FWO-TBM T001821N) granted to K.A., J.S. and B.B.. M.M. is supported by a KU Leuven Postdoctoral Mandate. J.P. is supported by the Marguerite-Marie Delacroix foundation and a postdoctoral fellowship of the Flanders Fund for Scientific Research (FWO; 1257621N).

The funding sources had no further role in study design; in the collection, analysis and interpretation of data; in the writing of the report; and in the decision to submit the paper for publication.

Statement of Ethics

This study protocol was reviewed and approved by the Ethics Committee for Biomedical Research at the University of Leuven, approval number [S61358]. Written informed consent from the parents and assent from the child were obtained prior to the study.

Corresponding author

Kaat Alaerts

KU Leuven, Neuromodulation Laboratory, Research Group for Neurorehabilitation, Tervuursevest 101 box 1501, 3001 Leuven, Belgium.

E-mail: kaat.alaerts@kuleuven.be

Tel.: +32 16 37 64 46

References

- (2013). World Medical Association Declaration of Helsinki: ethical principles for medical research involving human subjects. *Jama*, 310, 2191-2194.
- ALAERTS, K., DANIELS, N., MOERKERKE, M., EVENEPOEL, M., TANG, T., DONCK, S. V. D., CHUBAR, V., CLAES, S., STEYAERT, J., BOETS, B. & PRINSEN, J. (2023). At the head and heart of oxytocin's stress-regulatory neural and cardiac effects: a chronic administration RCT in children with autism. *medRxiv*, 2023.2004.2004.23288109.
- ALAERTS, K., TAILLIEU, A., PRINSEN, J. & DANIELS, N. (2021). Tracking transient changes in the intrinsic neural frequency architecture: Oxytocin facilitates non-harmonic relationships between alpha and theta rhythms in the resting brain. *Psychoneuroendocrinology*, 133, 105397.
- APA (1994). *DSM-IV. Diagnostic and Statistical Manual of Mental Disorders*. Washington DC: American Psychiatric Association.
- APA (2013). *Diagnostic and Statistical Manual of Mental Disorders*: American Psychiatric Association.
- BARTZ, J. A., ZAKI, J., BOLGER, N. & OCHSNER, K. N. (2011). Social effects of oxytocin in humans: context and person matter. *Trends Cogn Sci*, 15, 301-309.
- BRUINING, H., HARDSTONE, R., JUAREZ-MARTINEZ, E. L., SPRENGERS, J., AVRAMIEA, A. E., SIMPRAGA, S., HOUTMAN, S. J., POIL, S. S., DALLARES, E., PALVA, S., ORANJE, B., MATIAS PALVA, J., MANSVELDER, H. D. & LINKENKAER-HANSEN, K. (2020). Measurement of excitation-inhibition ratio in autism spectrum disorder using critical brain dynamics. *Sci Rep*, 10, 9195.
- CHENG, Y. C., HUANG, Y. C. & HUANG, W. L. (2020). Heart rate variability in individuals with autism spectrum disorders: A meta-analysis. *Neurosci Biobehav Rev*, 118, 463-471.
- CONSTANTINO, J. N., DAVIS, S. A., TODD, R. D., SCHINDLER, M. K., GROSS, M. M., BROPHY, S. L., METZGER, L. M., SHOUSHARI, C. S., SPLINTER, R. & REICH, W. (2003). Validation of a brief quantitative measure of autistic traits: Comparison of the social responsiveness scale with the autism diagnostic interview-revised. *Journal of Autism and Developmental Disorders*, 33, 427-433.
- DANIELS, N., MOERKERKE, M., STEYAERT, J., BAMP, A., DEBBAUT, E., PRINSEN, J., TANG, T., VAN DER DONCK, S., BOETS, B. & ALAERTS, K. (2023). Effects of multiple-dose intranasal oxytocin administration on social responsiveness in children with autism: a randomized, placebo-controlled trial. *Mol Autism*, 14, 16.
- DE BRUIJN, E. R. A., RUISSEN, M. I. & RADKE, S. (2017). Electrophysiological correlates of oxytocin-induced enhancement of social performance monitoring. *Soc Cogn Affect Neurosci*, 12, 1668-1677.
- EVENEPOEL, M., MOERKERKE, M., DANIELS, N., CHUBAR, V., CLAES, S., TURNER, J., VANAUDENAERDE, B., WILLEMS, L., VERHAEGHE, J., PRINSEN, J., STEYAERT, J., BOETS, B. & ALAERTS, K. (2023). Endogenous oxytocin levels in children with autism: Associations with cortisol levels and oxytocin receptor gene methylation. *Transl Psychiatry*, 13, 235.
- FATHABADIPOUR, S., MOHAMMADI, Z., ROSHANI, F., GOHARBAKHS, N., ALIZADEH, H., PALIZGAR, F., CUMMING, P., MICHEL, T. M. & VAFEE, M. S. (2022). The neural effects of oxytocin administration in autism spectrum disorders studied by fMRI: A systematic review. *J Psychiatr Res*, 154, 80-90.
- FESTANTE, F., FERRARI, P. F., THORPE, S. G., BUCHANAN, R. W. & FOX, N. A. (2020). Intranasal oxytocin enhances EEG mu rhythm desynchronization during execution and observation of social action: An exploratory study. *Psychoneuroendocrinology*, 111, 104467.
- FRIES, P. (2005). A mechanism for cognitive dynamics: neuronal communication through neuronal coherence. *Trends Cogn Sci*, 9, 474-480.
- GRACE, S. A., ROSSELL, S. L., HEINRICH, M., KORDSACHIA, C. & LABUSCHAGNE, I. (2018). Oxytocin and brain activity in humans: A systematic review and coordinate-based meta-analysis of functional MRI studies. *Psychoneuroendocrinology*, 96, 6-24.
- GUASTELLA, A. J., BOULTON, K. A., WHITEHOUSE, A. J. O., SONG, Y. J., THAPA, R., GREGORY, S. G., POKORSKI, I., GRANICH, J., DEMAYO, M. M., AMBARCHI, Z., WRAY, J., THOMAS, E. E. & HICKIE, I. B. (2023). The effect of oxytocin nasal spray on social interaction in young children with autism: a randomized clinical trial. *Mol Psychiatry*, 28, 834-842.
- HORTA, M., KAYLOR, K., FEIFEL, D. & EBNER, N. C. (2020). Chronic oxytocin administration as a tool for investigation and treatment: A cross-disciplinary systematic review. *Neurosci Biobehav Rev*, 108, 1-23.
- HUANG, Y., HUANG, X., EBSTEIN, R. P. & YU, R. (2021). Intranasal oxytocin in the treatment of autism spectrum disorders: A multilevel meta-analysis. *Neurosci Biobehav Rev*, 122, 18-27.
- JAIN, V., MARBACH, J., KIMBRO, S., ANDRADE, D. C., JAIN, A., CAPOZZI, E., MELE, K., DEL, R. R., KAY, M. W. & MENDELOWITZ, D. (2017). Benefits of oxytocin administration in obstructive sleep apnea. *Am. J. Physiol*

- Lung Cell Mol. Physiol*, 313, L825-L833.
- JOHNSON, M. H. (2017). Autism as an adaptive common variant pathway for human brain development. *Dev Cogn Neurosci*, 25, 5-11.
- JUREK, B. & NEUMANN, I. D. (2018). The Oxytocin Receptor: From Intracellular Signaling to Behavior. *Physiol Rev*, 98, 1805-1908.
- KEMP, A. H., QUINTANA, D. S., KUHNERT, R. L., GRIFFITHS, K., HICKIE, I. B. & GUASTELLA, A. J. (2012). Oxytocin increases heart rate variability in humans at rest: implications for social approach-related motivation and capacity for social engagement. *PLoS ONE*, 7, e44014.
- KLIMESCH, W. (2012). α -band oscillations, attention, and controlled access to stored information. *Trends Cogn Sci*, 16, 606-617.
- KLIMESCH, W. (2013). An algorithm for the EEG frequency architecture of consciousness and brain body coupling. *Front Hum. Neurosci*, 7, 766.
- KLIMESCH, W. (2018). The frequency architecture of brain and brain body oscillations: an analysis. *Eur J Neurosci*, 48, 2431-2453.
- LABORDE, S., MOSLEY, E. & THAYER, J. F. (2017). Heart rate variability and cardiac vagal tone in psychophysiological research - Recommendations for experiment planning, data analysis, and data reporting. *Frontiers in Psychology*. Frontiers Research Foundation.
- LORD, C., RUTTER, M., DILAVORE, P. C. & RISI, S. (1999). *Autism Diagnostic Observation Schedule*, Los Angeles: Western Psychological Service.
- MAIER, P., KAISER, M. E., GRINEVICH, V., DRAGUHN, A. & BOTH, M. (2016). Differential effects of oxytocin on mouse hippocampal oscillations in vitro. *Eur J Neurosci*, 44, 2885-2898.
- MARTINS, DAVIES, C., DE MICHELI, A., OLIVER, D., KRAWCZUN-RYGMACZEWSKA, A., FUSAR-POLI, P. & PALOYELIS, Y. (2020). Intranasal oxytocin increases heart-rate variability in men at clinical high risk for psychosis: a proof-of-concept study. *Transl Psychiatry*, 10, 227.
- MAZUREK, M. O., VASA, R. A., KALB, L. G., KANNE, S. M., ROSENBERG, D., KEEFER, A., MURRAY, D. S., FREEDMAN, B. & LOWERY, L. A. (2013). Anxiety, sensory over-responsivity, and gastrointestinal problems in children with autism spectrum disorders. *J Abnorm Child Psychol*, 41, 165-176.
- MOERKERKE, M., DANIELS, N., TIBERMONT, L., TANG, T., EVENEPOEL, M., VAN DER DONCK, S., DEBBAUT, E., PRINSEN, J., CHUBAR, V., CLAES, S., VANAUDENAERDE, B., WILLEMS, L., STEYAERT, J., BOETS, B. & ALAERTS, K. (2024). Chronic oxytocin administration stimulates the oxytocinergic system in children with autism. *Nature Communications*, 15, 58.
- MOERKERKE, M., DANIELS, N., VAN DER DONCK, S., TIBERMONT, L., TANG, T., DEBBAUT, E., BAMPS, A., PRINSEN, J., STEYAERT, J., ALAERTS, K. & BOETS, B. (2023). Can repeated intranasal oxytocin administration affect reduced neural sensitivity towards expressive faces in autism? A randomized controlled trial. *J Child Psychol Psychiatry*.
- NORMAN, G. J., CACIOPPO, J. T., MORRIS, J. S., MALARKEY, W. B., BERNTSON, G. G. & DEVRIES, A. C. (2011). Oxytocin increases autonomic cardiac control: moderation by loneliness. *Biol. Psychol*, 86, 174-180.
- OETTL, L. L., RAVI, N., SCHNEIDER, M., SCHELLER, M. F., SCHNEIDER, P., MITRE, M., DA SILVA, G. M., FROEMKE, R. C., CHAO, M. V., YOUNG, W. S., MEYER-LINDENBERG, A., GRINEVICH, V., SHUSTERMAN, R. & KELSCH, W. (2016). Oxytocin Enhances Social Recognition by Modulating Cortical Control of Early Olfactory Processing. *Neuron*, 90, 609-621.
- OWEN, S. F., TUNCDÉMIR, S. N., BADER, P. L., TIRKO, N. N., FISHELL, G. & TSIEN, R. W. (2013). Oxytocin enhances hippocampal spike transmission by modulating fast-spiking interneurons. *Nature*, 500, 458-462.
- PARKER, K. J., OZTAN, O., LIBOVE, R. A., SUMIYOSHI, R. D., JACKSON, L. P., KARHSON, D. S., SUMMERS, J. E., HINMAN, K. E., MOTONAGA, K. S., PHILLIPS, J. M., CARSON, D. S., GARNER, J. P. & HARDAN, A. Y. (2017). Intranasal oxytocin treatment for social deficits and biomarkers of response in children with autism. *Proc. Natl. Acad. Sci. U. S. A.*, 114, 8119-8124.
- PELTOLA, M. J., STRATHEARN, L. & PUURA, K. (2018). Oxytocin promotes face-sensitive neural responses to infant and adult faces in mothers. *Psychoneuroendocrinology*, 91, 261-270.
- PLETZER, B., KERSCHBAUM, H. & KLIMESCH, W. (2010). When frequencies never synchronize: the golden mean and the resting EEG. *Brain Res*, 1335, 91-102.
- QUINTANA, D. S. & GUASTELLA, A. J. (2020). An Allostatic Theory of Oxytocin. *Trends Cogn Sci*, 24, 515-528.
- RASSI, E., DORFFNER, G., GRUBER, W., SCHABUS, M. & KLIMESCH, W. (2019). Coupling and Decoupling between Brain and Body Oscillations. *Neuroscience Letters*, 711, 134401-134401.
- RODRIGUEZ-LARIOS, J. & ALAERTS, K. (2019). Tracking Transient Changes in the Neural Frequency Architecture: Harmonic Relationships between Theta and Alpha Peaks Facilitate Cognitive Performance. *J Neurosci*, 39, 6291-6298.

- RODRIGUEZ-LARIOS, J. & ALAERTS, K. (2020). EEG alpha-theta dynamics during mind wandering in the context of breath focus meditation: an experience sampling approach with novice meditation practitioners. *Eur J Neurosci*.
- RODRIGUEZ-LARIOS, J., FABER, P., ACHERMANN, P., TEI, S. & ALAERTS, K. (2020a). From thoughtless awareness to effortful cognition: alpha - theta cross-frequency dynamics in experienced meditators during meditation, rest and arithmetic. *Sci Rep*, 10, 5419.
- RODRIGUEZ-LARIOS, J., WONG, K. F., LIM, J. & ALAERTS, K. (2020b). Mindfulness Training is Associated with Changes in Alpha-Theta Cross-Frequency Dynamics During Meditation. *Mindfulness*, 11, 2695-2704.
- ROOPUN, A. K., KRAMER, M. A., CARRACEDO, L. M., KAISER, M., DAVIES, C. H., TRAUB, R. D., KOPELL, N. J. & WHITTINGTON, M. A. (2008). Temporal Interactions between Cortical Rhythms. *Front Neurosci*, 2, 145-154.
- RUBENSTEIN, J. L. & MERZENICH, M. M. (2003). Model of autism: increased ratio of excitation/inhibition in key neural systems. *Genes Brain Behav*, 2, 255-267.
- RUISSSEN, M. I. & DE BRUIJN, E. R. (2015). Is it me or is it you? Behavioral and electrophysiological effects of oxytocin administration on self-other integration during joint task performance. *Cortex*, 70, 146-154.
- RUTHERFORD, H. J. V., GUO, X. M., WU, J., GRABER, K. M., HAYES, N. J., PELPHREY, K. A. & MAYES, L. C. (2018). Intranasal oxytocin decreases cross-frequency coupling of neural oscillations at rest. *Int J Psychophysiol*, 123, 143-151.
- SCHILLER, B., KOENIG, T. & HEINRICH, M. (2019). Oxytocin modulates the temporal dynamics of resting EEG networks. *Sci Rep*, 9, 13418.
- SHAFFER, F., MCCRARY, R. & ZERR, C. L. (2014). A healthy heart is not a metronome: an integrative review of the heart's anatomy and heart rate variability. *Frontiers in Psychology*, 5.
- SHAMAY-TSOORY, S. G. & ABU-AKEL, A. (2016). The Social Salience Hypothesis of Oxytocin. *Biol. Psychiatry*, 79, 194-202.
- SINGH, F., NUNAG, J., MULDOON, G., CADENHEAD, K. S., PINEDA, J. A. & FEIFEL, D. (2016). Effects of intranasal oxytocin on neural processing within a socially relevant neural circuit. *Eur Neuropsychopharmacol*, 26, 626-630.
- SORIANO, J., DANIELS, N., PRINSEN, J. & ALAERTS, K. (2020). Intranasal oxytocin enhances approach-related EEG frontal alpha asymmetry during engagement of direct eye contact. *Brain Communications*.
- STOOP, R. (2012). Neuromodulation by oxytocin and vasopressin. *Neuron*, 76, 142-159.
- TARVAINEN, M. P., NISKANEN, J. P., LIPPONEN, J. A., RANTA-AHO, P. O. & KARJALAINEN, P. A. (2014). Kubios HRV-heart rate variability analysis software. *Comput Methods Programs Biomed*, 113, 210-220.
- TENKE, C. E. & KAYSER, J. (2005). Reference-free quantification of EEG spectra: combining current source density (CSD) and frequency principal components analysis (fPCA). *Clin Neurophysiol*, 116, 2826-2846.
- VAN DE CRUYS, S., EVERS, K., VAN DER HALLEN, R., VAN EYLEN, L., BOETS, B., DE-WIT, L. & WAGEMANS, J. (2014). Precise minds in uncertain worlds: predictive coding in autism. *Psychol Rev*, 121, 649-675.
- VAN DER DONCK, S., MOERKERKE, M., DLHOSOVA, T., VETTORI, S., DZHELIOVA, M., ALAERTS, K. & BOETS, B. (2022). Monitoring the effect of oxytocin on the neural sensitivity to emotional faces via frequency-tagging EEG: A double-blind, cross-over study. *Psychophysiology*, 59, e14026.
- WALLER, C., WITTFOTH, M., FRITZSCHE, K., TIMM, L., WITTFOTH-SCHARDT, D., ROTTLER, E., HEINRICH, M., BUCHHEIM, A., KIEFER, M. & GÜNDEL, H. (2015). Attachment representation modulates oxytocin effects on the processing of own-child faces in fathers. *Psychoneuroendocrinology*, 62, 27-35.
- WECHSLER, D. (1999). *Wechsler Abbreviated Scale of Intelligence (WASI)*, San Antonio, TX: Psychological Corporation.
- WIGTON, R., RADUA, J., ALLEN, P., AVERBECK, B., MEYER-LINDENBERG, A., MCGUIRE, P., SHERGILL, S. S. & FUSAR-POLI, P. (2015). Neurophysiological effects of acute oxytocin administration: systematic review and meta-analysis of placebo-controlled imaging studies. *J. Psychiatry Neurosci*, 40, E1-22.
- WYNN, J. K., GREEN, M. F., HELLEMANN, G., REAVIS, E. A. & MARDER, S. R. (2019). A dose-finding study of oxytocin using neurophysiological measures of social processing. *Neuropsychopharmacology*, 44, 289-294.
- YE, Z., STOLK, A., TONI, I. & HAGOORT, P. (2017). Oxytocin Modulates Semantic Integration in Speech Comprehension. *J Cogn Neurosci*, 29, 267-276.
- ZANINETTI, M. & RAGGENBASS, M. (2000). Oxytocin receptor agonists enhance inhibitory synaptic transmission in the rat hippocampus by activating interneurons in stratum pyramidale. *Eur J Neurosci*, 12, 3975-3984.
- ZELENINA, M., KOSILO, M., DA CRUZ, J., ANTUNES, M., FIGUEIREDO, P., MEHTA, M. A. & PRATA, D. (2022). Temporal Dynamics of Intranasal Oxytocin in Human Brain Electrophysiology. *Cereb Cortex*, 32, 3110-3126.
- ZHANG, X., LI, P., OTIENO, S., LI, H. & LEPPÄNEN, P. H. T. (2021). Oxytocin reduces romantic rejection-induced pain

in online speed-dating as revealed by decreased frontal-midline theta oscillations.
Psychoneuroendocrinology, 133, 105411.

Tables and Figures

Table 1

Demographic and clinical characteristics of children with and without autism, and of the children with autism randomized to receive oxytocin versus placebo. Data are presented as mean (\pm standard deviation). *P*-values correspond to independent sample t-tests or Chi-square tests assessing between-group differences in demographic scores between children with and without autism (first columns) and between children with autism, randomized to receive the oxytocin or placebo nasal spray (last columns).

Variable	Autism	Control	<i>p</i> value	Autism		<i>p</i> value
				Oxytocin	Placebo	
<i>n</i>	67	40		33	34	
Age (years)	10.49 \pm 1.28	10.28 \pm 1.32	0.43	10.6 \pm 1.32	10.36 \pm 1.25	0.43
Sex (M / F)	54 / 13	32 / 8	0.94	26 / 7	28 / 6	0.93
Verbal IQ	107.42 \pm 15.33	117.28 \pm 12.17	<0.01	105.79 \pm 14.89	109.06 \pm 15.83	0.39
Performance IQ	103.32 \pm 14.58	107.83 \pm 12.17	0.10	105.30 \pm 15.94	101.33 \pm 13.02	0.27
ADOS-2	/	/		9.43 \pm 3.96	9.67 \pm 4.31	0.83
SRS-2 Total	88.63 \pm 20.80	21.88 \pm 12.68	<0.01	88.03 \pm 22.54	89.21 \pm 19.29	0.82

The verbal intelligence quotient (IQ) was derived from the subtests Similarities and Vocabulary of the Wechsler Intelligence Scale for Children. The performance IQ was derived from the subtests Block design and Figure puzzles. ADOS-2: Autism Diagnostic Observation Schedule, 2nd edition. SRS-2: Social responsiveness Scale-Children, 2nd edition. M: male, F: female.

Figure 1

CONSORT flow diagram of participants in the trial.

EEG recordings were obtained at baseline (T0), after the four-week (oxytocin/placebo) nasal spray administration period (T1), and at a follow-up session, four weeks after cessation of the nasal spray administration period (T2). Data were analyzed using an intention-to-treat format with last-observations-carried-forward to replace missing data. Participants with missing baseline data were excluded list-wise. As outlined, for several participants, neural EEG assessments could not be acquired due to physical contact restrictions and closing down of hospital facilities during the COVID-19 pandemic.

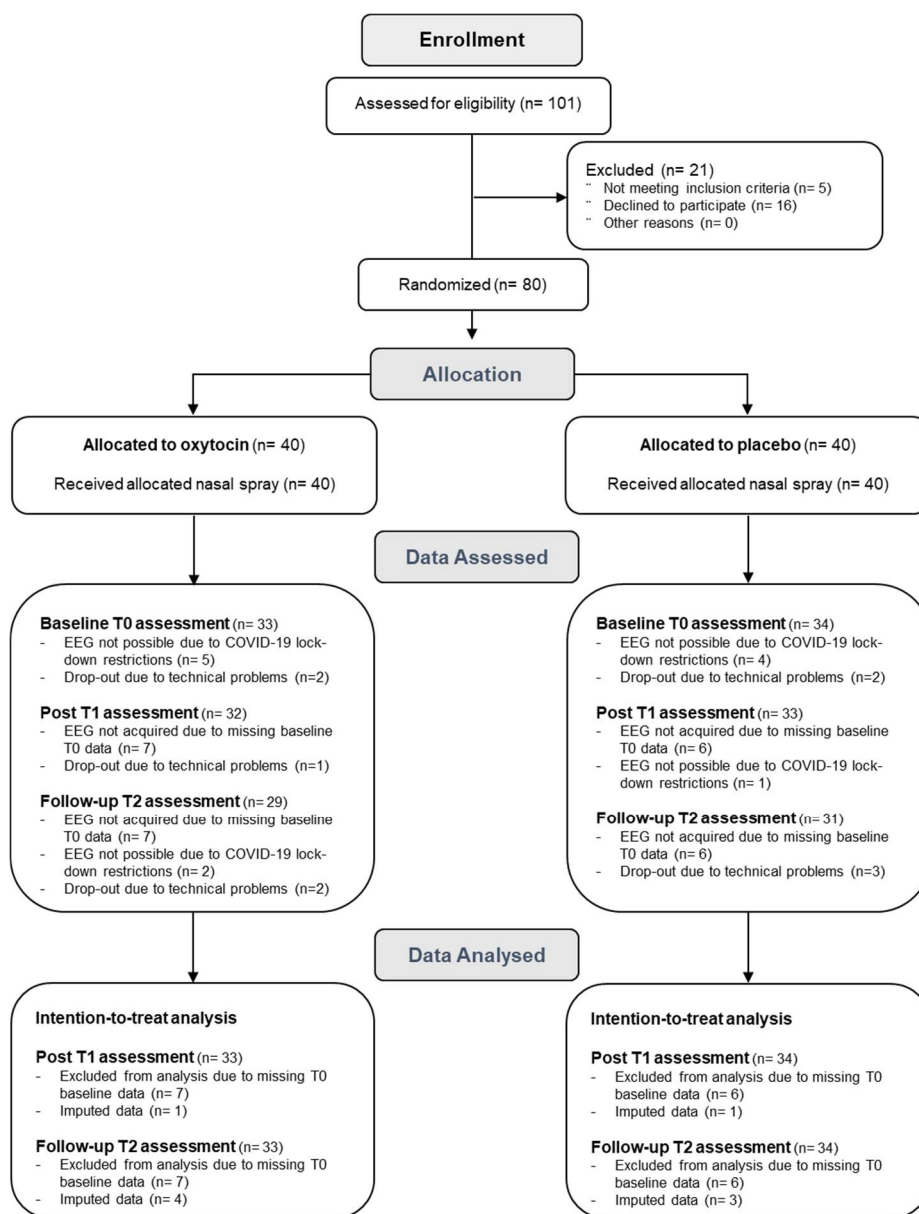


Figure 2

Transient detection of alpha and theta peak frequencies and determination of cross-frequency relationships.

Transient peak frequencies of the theta (4–8 Hz) and alpha (8–14 Hz) bands were detected within 1 sec epochs and the numerical ratio between the alpha and theta peak frequencies was calculated ($\text{peak-frequency}_{\text{alpha}}/\text{peak-frequency}_{\text{theta}}$).

A. Visualization of the transient (epoch-wise) variability of alpha and theta peak frequencies over time (i.e., 10 sec) for an exemplary subject, as well as the transient numerical ratio over time.

B. Visualization of the frequency spectra of two exemplary epochs in which the identified alpha and theta peak frequencies (indicated by asterisks) formed a harmonic (2:1) versus a nonharmonic (1.6:1) cross-frequency relationship. Visualizations are partly adapted from Alaerts et al. (2021).

C. Visualization of the relative occurrence of all possible cross-frequency relationship (proportion of epochs, averaged across electrodes) as recorded at baseline from children with and without autism. As visualized, a maximal occurrence of the non-harmonic 1.6:1 alpha:theta ratio aspect (9.46 %, average across electrodes) was evident. The harmonic 2:1 ratio aspect showed an average occurrence of 6.86% (average across electrodes).

D. As visualized, all reported cross-frequency analyses were computed within 11 distinct electrode clusters, encompassing left and right frontal (blue), central (green), parietal (red) and occipital (light blue) regions, as well as a midline frontal (light grey), central (mid grey) and occipital cluster (dark grey).

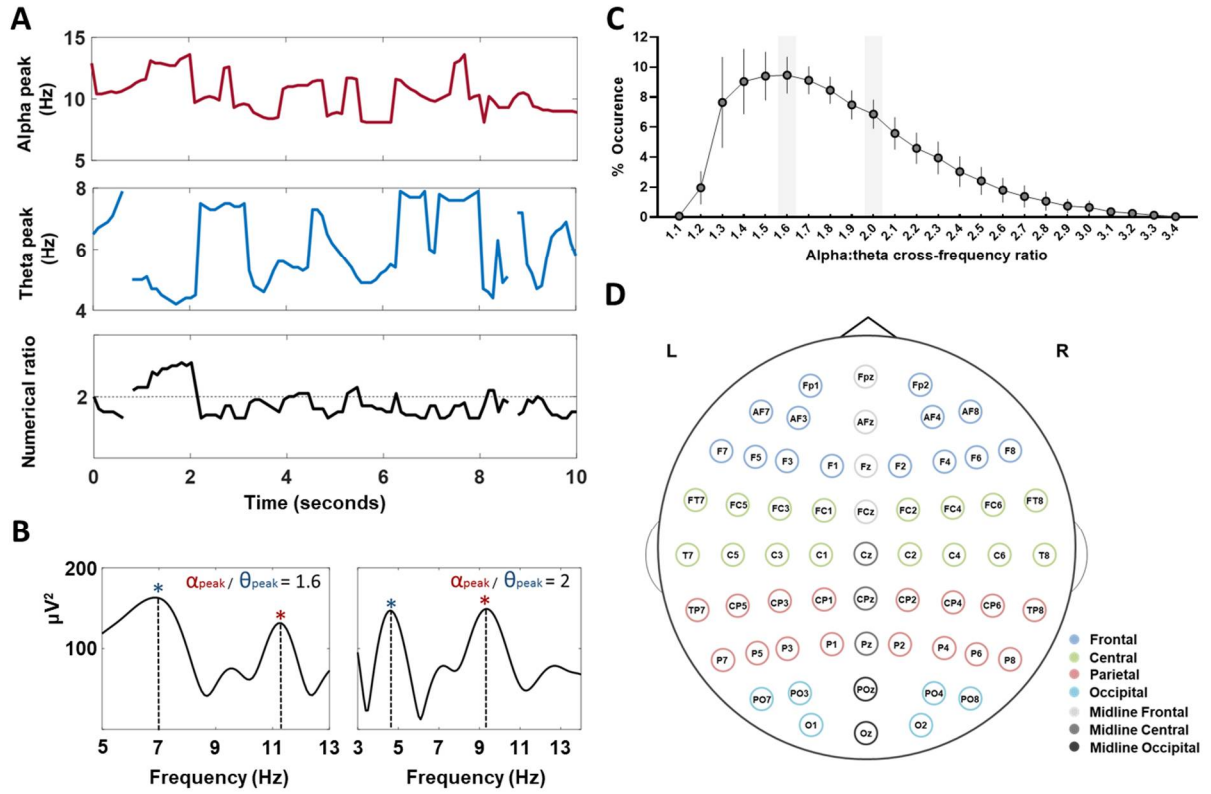


Figure 3

Diagnosis-related differences in EEG at baseline

Panel A visualizes individual data plots (with mean and standard deviation) of baseline diagnosis-related differences in the occurrence of the 1.6:1 'decoupling' non-harmonic (left plot) and 2:1 'coupling' harmonic ratio aspect (right plot). Data are visualized averaged across electrode clusters, separately for the group of children with ($n = 67$) and without autism (control; $n = 40$).

Panel B visualizes the relationship between baseline variations in high-frequency HRV and the baseline occurrence of the 1.6:1 'decoupling' non-harmonic (left plot), and the 2:1 'coupling' harmonic ratio aspect (right plot) in the group of children with autism ($n = 51$).

Panel C visualizes the relationship between baseline variations in social difficulties (assessed using the Social Responsiveness Scale, Total score) and the baseline occurrence of the 1.6:1 'decoupling' non-harmonic (left plot) and 2:1 'coupling' harmonic ratio aspect (right plot) in the group of children with autism ($n = 67$).

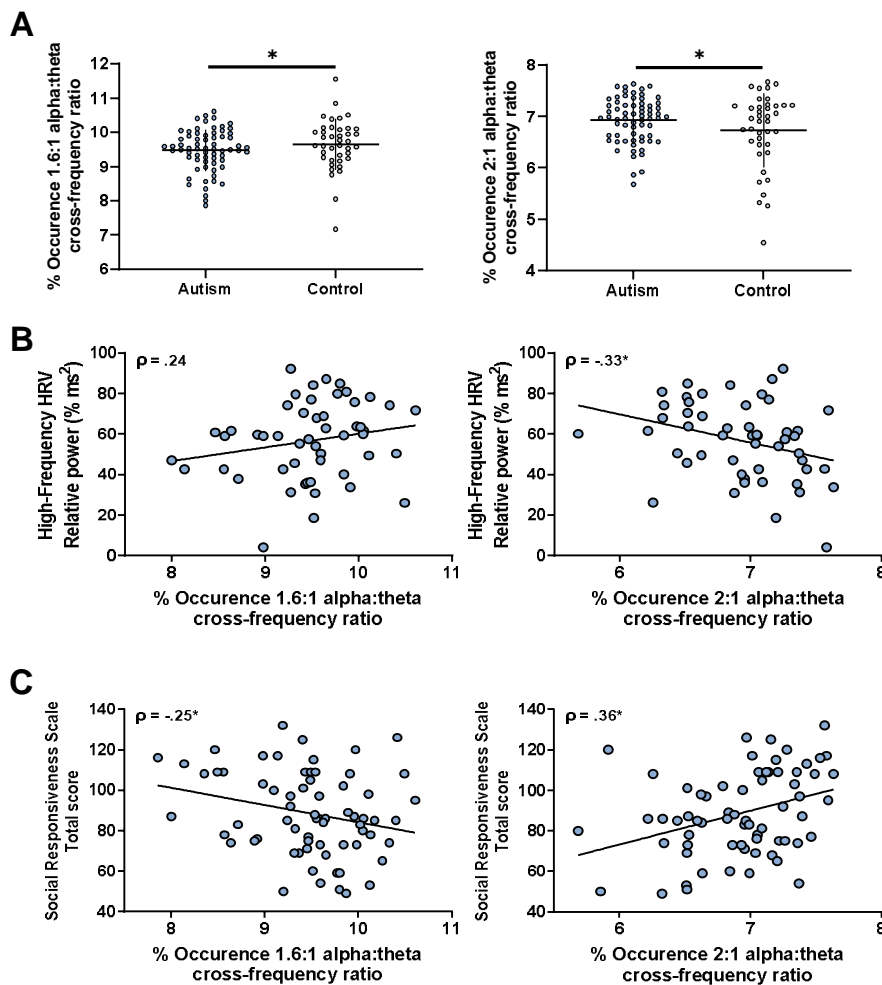


Figure 4

Oxytocin-induced changes in EEG and HRV

Panel A visualizes changes from baseline in the occurrence of the 1.6:1 'decoupling' non-harmonic and 2:1 'coupling' harmonic ratio aspect. Data are visualized separately for the oxytocin ($n = 33$) and placebo groups ($n = 34$), at post assessment session T1, immediately after the four-week nasal spray administration period, and at assessment session T2, four weeks after cessation of the nasal spray administration period. Data are visualized averaged across electrode clusters.

Panel B visualizes changes from baseline in high-frequency HRV separately for the oxytocin ($n = 27$) and placebo groups ($n = 23$), at post assessment session T1, and follow-up assessment T2.

Vertical lines denote standard error of the mean.

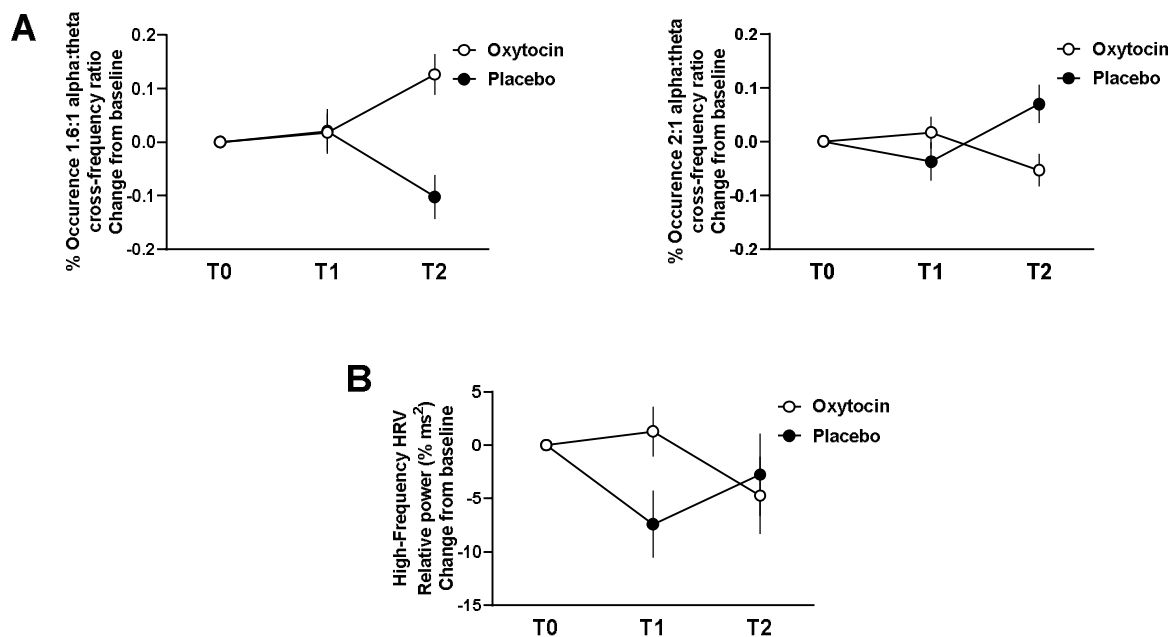
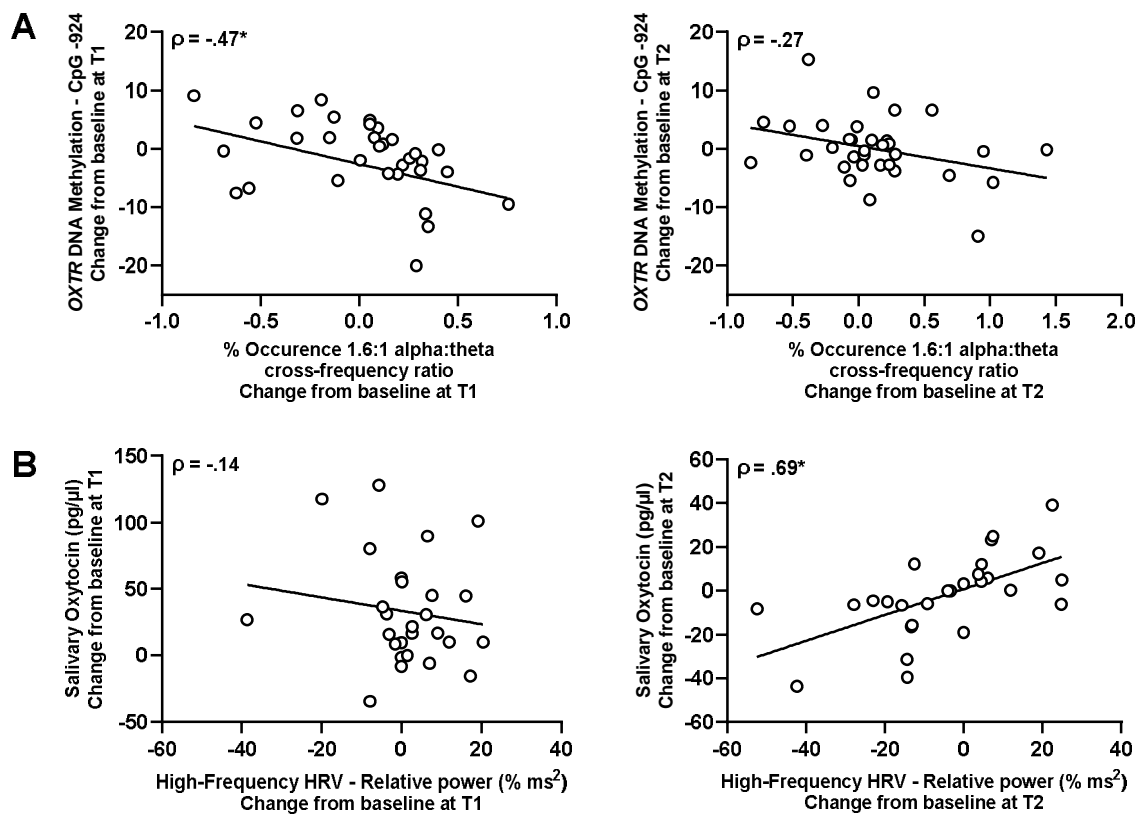


Figure 5

Association between oxytocin-induced changes in neural/cardiac and biological sampling parameters

Panel A visualizes the relationship between oxytocin-induced changes in *OXTR* methylation (at CpG site -924) and the occurrence of the 1.6:1 'decoupling' non-harmonic ratio aspect, at the T1 immediate post assessment session (left plot, $n = 33$) and at the T2 follow-up assessment session (right plot, $n = 33$).

Panel B visualizes the relationship between oxytocin-induced changes in salivary oxytocin levels and high-frequency HRV at the T1 immediate post assessment session (left plot, $n = 27$) and at the T2 follow-up assessment session (right plot, $n = 27$).



Supplementary Material

Chronic oxytocin improves neural decoupling at rest in children with autism: An exploratory RCT

Alaerts Kaat *, Moerkerke Matthijs*, Daniels Nicky*, Zhang Qianqian, Steyaert Jean, Ricchiuti Grazia, Prinsen Jellina †, Boets Bart †

* Joint first authors

† Joint senior authors

Supplementary Methods

Nasal spray compliance monitoring.

To monitor nasal spray compliance, the total amount of administered fluid was assessed. Generally compliance was high with no significant differences between the total amount of administered fluid in the oxytocin and placebo administration groups (oxytocin: 14.86 ± 2.37 ml; placebo: 13.79 ± 2.35 ml; $t(75) = 2.00$, $p = .050$).

Compliance to the use of the nasal spray was also assured using a daily medication diary that recorded date and time of administration (oxytocin: $96.75 \pm 5.26\%$; placebo: $96.11 \pm 5.29\%$; $t(74) = .52$, $p = .603$).

Assessment of salivary oxytocin levels

Oxytocin levels were assessed via saliva samples acquired at each assessment session (T0, T1, T2), using Salivette cotton swabs (Sarstedt AG & Co., Germany) and analysed using enzyme immunoassay oxytocin ELISA kits (Enzo Life Sciences, Inc., USA) in accordance with the manufacturer's instructions. Sample concentrations samples (100 μ l/well) were calculated conform plate-specific standard curves. More detailed information regarding the salivary assessment procedures, data handling and analyses are provided in ^{1,2}.

In short, oxytocin levels, acquired at home, within 30 min after awakening and before breakfast showed strong oxytocin-induced changes, particularly at the T1 immediate post-session ². In the current report, it was examined whether these changes in endogenous oxytocin levels were associated to oxytocin-induced changes in the assessed neural EEG and cardiac HRV parameters.

Salivary oxytocin level data were obtained from all analysed participants of the oxytocin group (i.e., $n = 33$; see CONSORT flow diagram, **Figure 1**).

Assessment of OXTR DNA methylation levels

To assess variations in DNA methylation of *OXTR* (hg19, chr3:8,810,729-8,810,845), salivary samples were obtained via the Oragene DNA sample collection kit (DNA Genotek Inc., Canada) at the Leuven University hospital (i.e. at T0, T1, T2). More detailed information regarding the DNA collection procedures, data handling and analyses are provided in ^{1,2}.

In short, of the three assessed CpG sites (-934, -924 and -914), CpG -924 showed reliable oxytocin-induced changes, indicating a reduction in *OXTR* methylation at this site, both immediately post and at the four-week follow-up, indicating sustained epigenetic modifications that facilitate heightened oxytocin receptor expression ². In the current report, it was examined whether epigenetic changes at this site were associated to oxytocin-induced changes in the assessed neural EEG and cardiac HRV parameters.

Salivary epigenetic samplings were obtained from all analysed participants of the oxytocin group (i.e., $n = 33$; see CONSORT flow diagram, **Figure 1**).

Secondary EEG analyses

Oxytocin-induced changes in alpha and theta peak frequencies. Mean peak frequencies of the alpha (8–14 Hz) and theta band (4–8 Hz) were estimated by averaging the peak frequency of transiently detected peaks over time. To examine oxytocin-induced effects, pre-to-post changes in alpha and theta peak frequencies were subjected to separate mixed-effect models, with the random factor ‘subject’ and the fixed factors ‘nasal spray’ (oxytocin, placebo), ‘assessment session’ (T1, T2), and ‘electrode cluster’ (11 clusters).

Oxytocin-induced changes in alpha and theta power amplitude estimations. Secondary analyses were performed to explore whether estimations of alpha and theta absolute power amplitudes showed oxytocin-related changes. After obtaining the time-frequency representation through the MATLAB *spectrogram* function (window length of 1 sec; 90.23 % overlap, 0.1 Hz resolution between 1 and 30 Hz), absolute amplitudes (in μV) of the alpha (8–14 Hz) and theta band (4–8 Hz) were estimated.

Pre-to-post changes in alpha and theta absolute amplitudes were subjected to separate mixed-effect models, with the random factor ‘subject’ and the fixed factors ‘nasal spray’ (oxytocin, placebo), ‘assessment session’ (T1, T2), and ‘electrode cluster’ (11 clusters).

Supplementary Results

Nasal spray compliance monitoring

Compliance was overall high with no significant differences between the total amount of administered fluid in the oxytocin compared to the placebo group (oxytocin: 14.86 ± 2.37 ml; placebo: 13.79 ± 2.35 ml; $t(75) = 2.00$, $p = .050$). Compliance to the use of the nasal spray was also assured using a daily medication diary that recorded date and time of administration (oxytocin: $96.75 \pm 5.26\%$; placebo: $96.11 \pm 5.29\%$; $t(74) = .52$, $p = .603$) (see also Daniels et al. 2023³).

EEG cross-frequency and high-frequency HRV analyses on data without imputation

Secondary analyses were performed on EEG and high-frequency HRV data without imputation to examine the robustness of the identified oxytocin-induced changes within the primary analyses (with imputation). To do so, available data were subjected to similar mixed-effect analyses which can handle moderate amounts of missing data (i.e., missing data from 2 participants at T1, and data from 7 participants at T2, see CONSORT flow diagram, **Figure 1**).

EEG cross-frequency dynamics. In line with the primary analyses (with imputation), mixed-effect analyses on data without imputation yielded a significant ‘nasal spray x cross-frequency ratio x session’ interaction ($F(1, 2597) = 8.65$; $p < .001$), indicating a qualitatively similar pattern of results with or without imputation of missing data points.

HRV stress physiology. High-frequency HRV analyses on data without imputation also revealed a similar ‘nasal spray x session’ interaction ($F(1, 48.852) = 6.44$; $p = .014$), indicating robustness to the imputation method.

Diagnosis-related differences and oxytocin-induced changes in low-frequency HRV

Diagnosis-related differences. As a group, low-frequency HRV was not significantly different between children with and without autism ($t(81) = -.78$; $p = .43$).

Oxytocin-induced changes. Mixed-effect analyses of pre-to-post changes in low-frequency HRV revealed a significant ‘nasal spray x session’ interaction ($F(1, 48) = 4.58$; $p = .037$), indicating that,

compared to the placebo group, children receiving oxytocin displayed significantly *lower* low-frequency HRV at the T1 post session, compared to the placebo group, (post-hoc: $p_{Fisher\ LSD} = .027$; $p_{Bonferroni} = .16$), but no longer at the T2 session (post-hoc: $p_{Fisher\ LSD} = .46$; $p_{Bonferroni} > 1.0$).

Accordingly, while the exact nature of the low-frequency HRV component is not fully clear (likely emerging from a combinatory influence of the parasympathetic and sympathetic autonomic nervous system ⁴, as well as reflective of baroreceptor regulation ⁵), it appears that oxytocin primarily induced a down-regulation of low-frequency HRV power, while facilitating an overall upregulation of the parasympathetically driven high-frequency HRV index.

Secondary EEG analyses of alpha and theta peak frequencies and power amplitudes

Alpha and theta peak frequencies. In the primary analyses, oxytocin-induced differences in the occurrence of 1.6:1 and 2:1 ratio aspects were assessed. Secondary analyses were performed to explore whether similar oxytocin-related differences are evident when mean alpha and theta peak frequencies are analyzed separately.

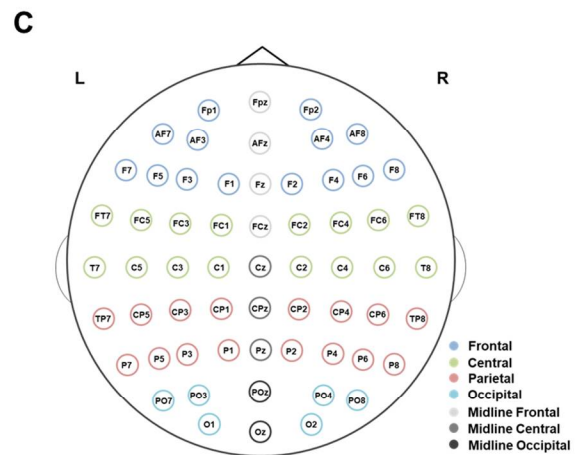
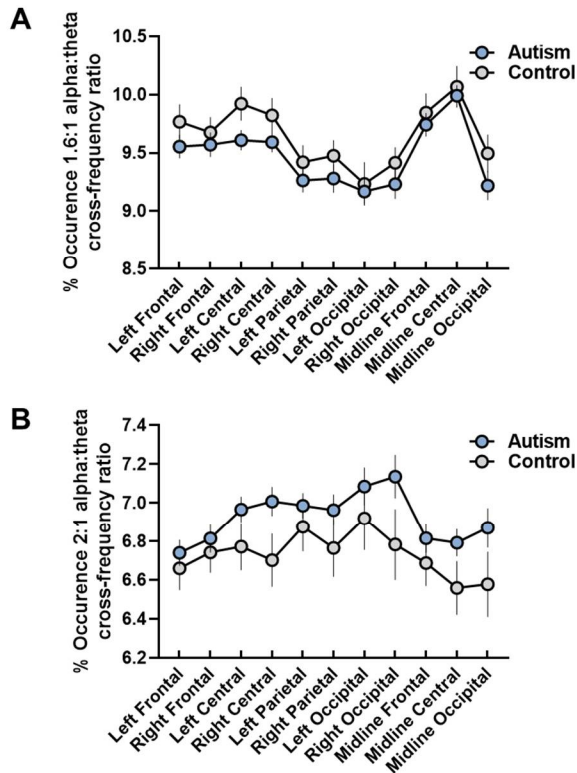
Mixed-effect analyses on pre-to-post changes in theta peak frequencies yielded a significant 'nasal spray x session' interaction effect ($F(1, 48) = 4.77$; $p = .034$), indicating that across electrode clusters, children receiving placebo displayed a stronger decrease in theta peak frequencies, compared to children receiving oxytocin, only at the T2 four-week follow-up session ($p_{Bonferroni} < .001$), not at the T1 session ($p_{Bonferroni} > 1.0$). Notably, across groups and both at the T1 and T2 session, stronger decreases in theta peak frequencies were associated with a reduced formation of 1.6:1 non-harmonic ratio aspects (across groups: T1: $\rho = .40$; $p < .001$; T2: $\rho = .46$; $p < .001$). Inversely, increases in alpha peak frequencies were associated with a decreased formation of 1.6:1 non-harmonic ratio aspects (T1: $\rho = -.26$; $p = .036$; T2: $\rho > -.32$; $p = .01$), although note that mixed-effect analyses of changes in alpha peak frequencies revealed no main or interaction effects with the factor 'nasal spray' (all, $p > .05$).

Alpha and theta absolute power amplitudes. Mixed-effect analyses on pre-to-post changes in theta or alpha power amplitudes revealed no significant main or interaction effects with the factor 'nasal spray' (all, $p > .05$), indicating no differential effect of oxytocin versus placebo nasal spray on resting spectral power.

Supplementary Figure 1

Diagnosis-related differences in EEG cross-frequency dynamics, separately for electrode clusters

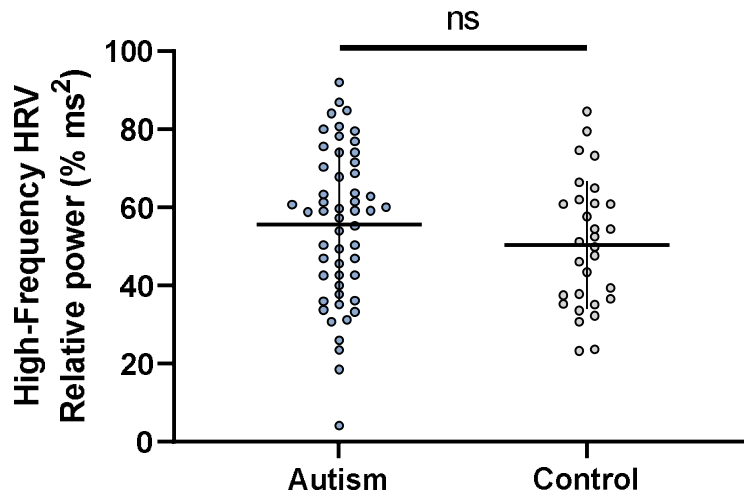
Baseline diagnosis-related differences in the occurrence of the 1.6:1 non-harmonic (panel A) and 2:1 harmonic ratio aspect (panel B) are visualized separately each electrode cluster (11, see panel C). Data are visualized separately for the group of children with and without autism (control).



Supplementary Figure 2

Diagnosis-related differences in high-frequency HRV at baseline

Individual data plots (with mean and standard deviation) are visualized of baseline diagnosis-related differences in high-frequency HRV. Data are visualized separately for the group of children with and without autism (control).



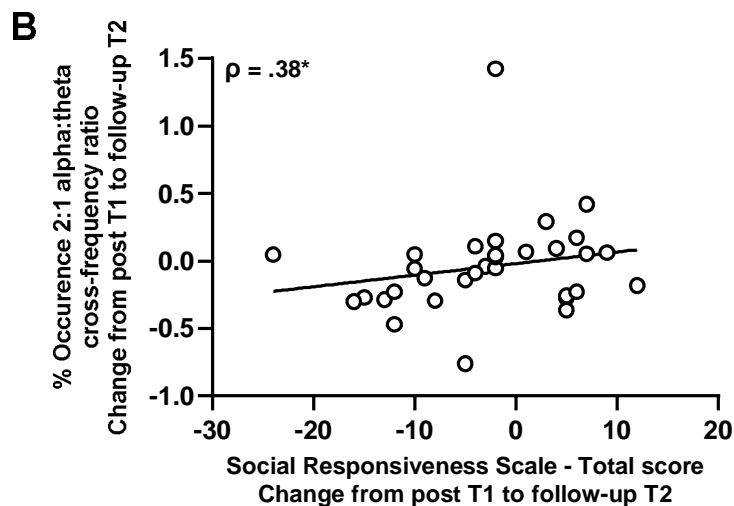
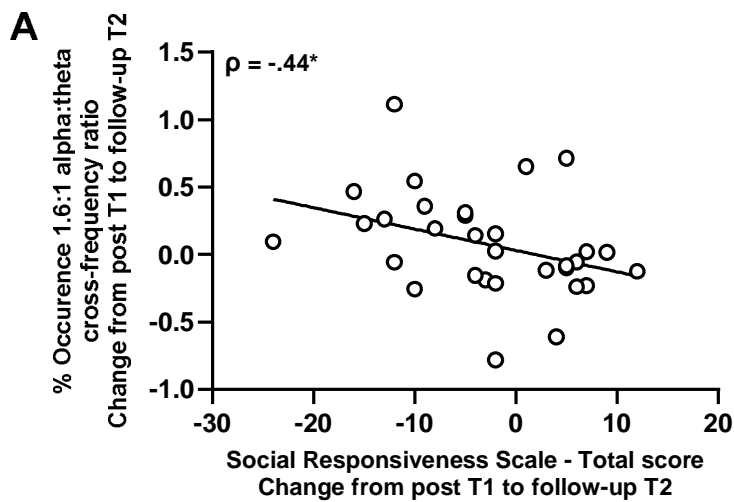
Supplementary Figure 3

Association between late-emerging oxytocin-induced changes (from post T1 to follow-up T2) in neural and behavioral parameters.

Panel A visualizes the relationship between late-emerging oxytocin-induced changes (from post T1 to follow-up T2) in the occurrence of the 1.6:1 ‘decoupling’ non-harmonic ratio aspect and changes (from post T1 to follow-up T2) in social difficulties (assessed using the Social Responsiveness Scale, SRS Total score) ($n = 32$).

Panel B visualizes the relationship between late-emerging oxytocin-induced changes (from post T1 to follow-up T2) in the occurrence of the 2:1 ‘coupling’ harmonic ratio aspect and changes (from post T1 to follow-up T2) in SRS Total scores ($n = 32$). Note that lower SRS Total scores denote improvement in social function.

Together, these relationships indicated that participants with stronger late-emerging oxytocin-induced increases in 1.6:1 non-harmonic cross-frequency coupling, and stronger late-emerging decreases in 2:1 harmonic cross-frequency coupling (from T1 to T2), showed more pronounced improvements in SRS social function (from T1 to T2).



References

1. Evenepoel, M., *et al.* Endogenous oxytocin levels in children with autism: Associations with cortisol levels and oxytocin receptor gene methylation. *Transl Psychiatry* **13**, 235 (2023).
2. Moerkerke, M., *et al.* Chronic oxytocin administration stimulates the endogenous oxytocin system: an RCT in autistic children. *medRxiv*, 2023.2006.2006.23291017 (2023).
3. Daniels, N., *et al.* Effects of multiple-dose intranasal oxytocin administration on social responsiveness in children with autism: a randomized, placebo-controlled trial. *Mol Autism* **14**, 16 (2023).
4. Goldstein, D.S., Benthoo, O., Park, M.Y. & Sharabi, Y. Low-frequency power of heart rate variability is not a measure of cardiac sympathetic tone but may be a measure of modulation of cardiac autonomic outflows by baroreflexes. *Exp Physiol* **96**, 1255-1261 (2011).
5. Shaffer, F. & Ginsberg, J.P. An Overview of Heart Rate Variability Metrics and Norms. *Frontiers in Public Health* **5**(2017).